AMERICAN UNIVERSITY OF BEIRUT

INFLUENCE OF LOADING RATES ON SINGLE SHEAR-BOLTED LAP JOINTS IN FIRE

by
RAYAN ALI CHAHROUR

A thesis
submitted in partial fulfillment of the requirements
for the degree of Master of Engineering
to the Department of Civil and Environmental Engineering
of the Maroun Semaan Faculty of Engineering and Architecture
at the American University of Beirut

Beirut, Lebanon
September 2020

AMERICAN UNIVERSITY OF BEIRUT

INFLUENCE OF LOADING RATES ON SINGLE SHEAR-BOLTED LAP JOINTS IN FIRE

by

RAYAN ALI CHAHROUR

Approved by:

Dr. Elie G. Hantouche, Associate Professor — Advisor
Department of Civil and Environmental Engineering

Dr. Mayssa Dabaghi, Assistant Professor — Member of Committee
Department of Civil and Environmental Engineering

Dr. Salah Sadek, Professor — Member of Committee
Department of Civil and Environmental Engineering

Date of thesis defense: September 04, 2020

AMERICAN UNIVERSITY OF BEIRUT

THESIS, DISSERTATION, PROJECT RELEASE FORM

Student Name: Chahrour Rayan Ali
Last First Middle

● Master's Thesis ○ Master's Project ○ Doctoral Dissertation

☐ I authorize the American University of Beirut to: (a) reproduce hard or electronic copies of my thesis, dissertation, or project; (b) include such copies in the archives and digital repositories of the University; and (c) make freely available such copies to third parties for research or educational purposes.

☑ I authorize the American University of Beirut, to: (a) reproduce hard or electronic copies of it; (b) include such copies in the archives and digital repositories of the University; and (c) make freely available such copies to third parties for research or educational purposes
after : **One ✓ year from the date of submission of my thesis, dissertation, or project.**
Two ---- years from the date of submission of my thesis, dissertation, or project.
Three ---- years from the date of submission of my thesis, dissertation, or project.

Rayan Chahrour Sep. 10, 2020
Signature Date

ACKNOWLEDGMENTS

I would like to express my deep gratitude to my thesis advisor Dr. Elie Hantouche for his continuous support, patience, and guidance throughout my study. I value his constant dedication and enthusiasm which lead to the successful development of this research work. His knowledge and expertise are the bedrocks that helped my research skills grow throughout my time spent at the American University of Beirut.

My recognition and gratitude are also extended to my thesis committee Dr. Mayssa Dabaghi and Dr. Salah Sadek. I would also like to thank PhD candidate Ahmad El Ghor for his help, support, and assistance throughout my study.

Furthermore, I would like to acknowledge the financial support provided by the American University of Beirut Research Board under Award No. 103780-24705.

Finally, I must express my profound gratitude to both of my parents, brother, sisters, and friends. I would also like to thank my research team for all their help and support for the past two years. This accomplishment would not have been possible if it were not for your unlimited support. Thank you.

AN ABSTRACT OF THE THESIS OF

Rayan Ali Chahrour for Master of Engineering
Major: Civil and Environmental Engineering

Title: Influence of Loading Rates on Single Shear-Bolted Lap Joints in Fire

The objective of this research is to investigate the effect of loading rates or implicit creep on the strength and deformation capacities of single shear-bolted lap joints and shear tab connections at elevated temperatures. To address this issue, sixteen single shear-bolted lap joints were tested under two different loading rates for temperatures ranging from 400°C to 700°C. The rate- and the temperature-dependent retention factors for the bolt shear capacities were presented and compared with previous studies available in the literature. The effect of loading rate and temperature on the bolt pretension force were also examined. The results show that all tested bolted lap joints failed in bolt shear. Also, the results of the slow loading rate tests showed a larger reduction in the bolt shear capacities when compared to the fast tests for temperatures larger than 400°C. That is, the effect of loading rate on the bolt shear capacity ranges from 18% to 36% difference for temperatures ranging from 450°C to 700°C, respectively. Finally, a strength reduction coefficient was introduced in the bolt shear capacity equation to account for the loading rate effect when designing bolted connections in fire.

Finite Element (FE) models were developed and validated against the performed experimental program and others available in the literature. The models studied the behavior, strength capacities and failure modes of bolted lap joints and shear tab connections at elevated temperatures with and without the thermal creep effect. The results showed that the thermal creep effect changes the failure mode and decreases the bolt strength capacities of bolted connections at elevated temperatures.

Finally, a step-by-step fire design procedure and an example of an isolated shear tab connection were presented. The design includes the thermal creep effect by incorporating the developed strength reduction coefficient in the bolt shear capacity equation. The outcome showed that adding the effect of thermal creep decreases the capacity of the connection by 40% at 500°C.

This research shows that considering the effect of thermal creep when designing bolted connections during fire is essential for structural fire-engineering applications. Including this effect provides more precise prediction of their behavior.

CONTENTS

ILLUSTRATIONS

TABLES

LIST OF ABBREVIATIONS

A_b	Effective area of the bolt shank, in^2
A_{gv}	Gross area subject to shear for block shear failure mode, in^2
A_{nt}	Net area subject to tension for block shear failure mode, in^2
A_{nv}	Net area subject to shear for block shear failure mode, in^2
A_s	Effective shear area, in^2
$A_{s,net}$	Net effective shear area, in^2
A_{we}	Effective area of the weld, in^2
D_u	Ratio of the mean installed bolt pretension to the specified minimum bolt pretension
F_{EXX}	Filler metal classification strength at ambient temperature, ksi
F_{nv}	Nominal shear strength of steel bolt at ambient temperature, ksi
F_{ut}	Ultimate strength of base material at ambient temperature, ksi
F_{yt}	Yield strength of base material at ambient temperature, ksi
I_{weld}	Moment of inertia about the x-axis of fillet weld, in^4
K_{bt}	Temperature-dependent retention factor for the ultimate strength of steel bolt
K_{ut}	Temperature-dependent retention factor the ultimate strength of the base material
K_{wt}	Temperature-dependent retention factor for the ultimate strength of the weld
K_{yt}	Temperature-dependent retention factor the yield strength of the base material
K_{PT}	Temperature-dependent retention factor for the pretension force
L_{eh}	Horizontal edge distance, in
L_{ev}	Vertical edge distance, in
M	Resultant moment on the connection calculated from applied shear and tensile forces, kip-in
M_u	Rupture moment capacity, kip-in
M_y	Yielding moment capacity, kip-in
P	Axial force due to thermal expansion of the beam, kips

R_{br}	Strength of plate/beam web in bearing/tear-out, kips
R_{BS}	Block shear capacity, kips
R_{nw}	Weld strength, kips
R_s	Bolt slip resistance at elevated temperatures, kips
R_v	Bolt shear resistance, kips
R_{vy}	Shear yielding of the shear tab plate, kips
R_{vu}	Shear rupture of the shear tab plate, kips
R_t	Bolt tensile resistance, kips
S_x	Elastic section modulus about the x-axis, in^3
T	Temperature, °C
T_b	Minimum pretension force applied on the bolt, kips
U_{bs}	Tension stress distribution factor
V	Applied shear force on the connection, kips
V_{bottom}	Applied shear force on the bottom bolt, kips
V_m	Bolt shear forces due to applied moment, kips
V_{middle}	Applied shear force on the middle bolt, kips
V_p	Bolt shear forces due to compressive force, kips
V_{top}	Applied shear force on the top bolt, kips
V_v	Bolt shear forces due to gravity load, kips
Z_{net}	Net plastic section moduli about the x-axis, in^3
Z_x	Plastic section moduli about the x-axis, in^3
a	Distance from the bolt line to the weld line, in
d_b	Diameter of bolt shank, in
e	Shear force eccentricity, in
f_t	Shear stress perpendicular and parallel to the weld line, ksi
f_v	Shear stress parallel to the weld line, ksi
h	Distance between the end components connecting shear tab to column, in
h_f	Factor of fillers
l_c	Clear distance between the edge of the bolt hole and the edge of the material, in

n_s	Number of slip/shear planes
p	Distance between the farthest bolt-row and center of rotation ‘c’, in
t	Thickness of shear tab plate or beam web, in
t_{max}	Maximum thickness of shear tab plate or beam web, in
w	Thickness of fillet weld, in
w_{min}	Minimum allowable thickness of fillet weld, in
μ	Mean slip coefficient for Class A or B surfaces
α	Shear bolt strength reduction coefficient
θ	Angle between the line of action of the required force and the weld longitudinal axis, degrees

CHAPTER I

INTRODUCTION

Structural steel members are commonly used in the construction industry especially in high rise buildings and long span bridges. This structural material is favored due to their mechanical properties and ease in construction and repair. These structures are susceptible of being exposed to fire disasters which lead to their material degradation, partial failure, and in some cases total collapse. Therefore, understanding the behavior of steel structures at elevated temperatures is essential to develop safe and reliable design guidelines for fire-engineering practice.

In steel buildings, the structural elements are connected using different types of simple bolted and welded connections specifically designed to transfer gravity loads. Structural bolts play a crucial role in transferring these applied loads between the connected components of a bolted connection. This role becomes more critical during fire. The steel floor-beams expand during the heating phase and contracts during the cooling phase, and thus developing additional axial forces and moments on the beam-end connections called the “thermal-induced forces”. In fact, these thermal-induced forces imposed on simple connections were one of the reasons that the fires developed in WTC 7 lead to total collapse (NIST, 2008). Also, bolts exhibit a rapid reduction in strength as compared to the conventional steel when temperatures exceed 400°C (Kodur et al. 2012). These aforementioned factors combined can alter the controlling failure mode of bolted connections from beam web tear-out or block shear to bolt shear failure when subjected to elevated temperatures (Yu et al. 2009; Hu and Engelhardt 2012). In addition to these factors, the behavior of bolted connections can be affected by the rate at which the fire-induced load is applied (implicit creep). Therefore,

understanding the behavior of bolted connections in a fire event requires accurate knowledge of the time and thermal behavior of bolts subjected to shear forces, which can be crucial for designing such connections in fire.

Bolt shear failure is a governing failure mode in bolted connections, especially when subjected to elevated temperatures. Experimental results showed that when M24 Grade 10.9 bolts were used in fin plate connections, the failure was due to block shear of the beam web at ambient temperature and changed to bolt shear failure at 550°C (Yu et al. 2009). Also, experimental tests on a shear tab connection showed that the failure mode changed from bearing to bolt shear failure at 400°C and 500°C for tests subjected to inclined and pure tension, respectively (Hu and Engelhardt 2012). This indicates that bolt shear failure can govern the connection response during fire and understanding its rate and thermal behavior are of great importance.

Previous experimental studies also investigated the effect of geometric properties and elevated temperatures on the material degradation and load-bearing behavior of structural bolts and bolted lap joint in fire (Kirby 1995; Yu 2006; Hanus et al. 2011; Yang et al. 2011; Kodur et al. 2012; Hirashima et al. 2014; Fischer et al. 2018; Peixoto et al. 2017). These studies showed the degradation of the bolt strength capacity when subjected to elevated temperatures. For instance, experimental tests were performed on Grade 8.8 bolts subjected to tension and double shear under elevated temperatures up to 800°C (Kirby 1995). The results showed a significant loss of bolt strength when subjected to temperatures larger than 300°C. The retention factors for the bolt strength capacities presented by Kirby (1995) were adopted by Eurocode 3 (2005) (Yang et al. 2011). Also, those present in Eurocode 3 (2005) are available in the AISC 360 *Appendix 4* (2016). Tensile tests were also performed on two types of coupon high-strength bolts materials: A325 and A490 that showed the decrease in ultimate strength

capacity by 92% at 700°C (Kodur et al. 2012). Experimental tests were also performed on single-bolted lap joints showing the effect of bolt diameter, plate thickness, and temperature on their failure modes and behavior (Fischer et al. 2018).

In addition to the experimental programs, previous FE analysis were also conducted to study the behavior of shear tab connections subjected to elevated temperatures. Finite element studies were performed to propose simple modifications on shear tab connections that improve their behavior during a fire (Garlock and Selamet 2010). Also, finite element simulations were performed to study the effect of elevated temperatures on the failure modes and behavior of shear tab connections (Seif et al. 2013, 2016). The results showed that the change in failure mode in shear tab connections during fire occurs due to two factors namely: the degradation of the steel material, and the deformations prior to fracture due to the thermal expansion and contraction. A previous study also developed a mechanical model that predicts the effect of explicit creep on the rotational stiffness and the strength of shear tab connections in fire (Jabotian and Hantouche, 2019). Finally, a stiffness-based model was also developed that predicts the rotational stiffness and capacity of shear tab and double-angle connections at elevated temperatures (Hantouche et al. 2020). Then, this model was used to provide fire-design examples on a shear tab connection and on a double-angle connection.

All the previous studies on bolts, bolted lap joints and shear tab connections investigated the effect of material and some geometric parameters on the bolted connections behavior at elevated temperatures. However, none of these studies considered the effect of loading rates or thermal creep on the behavior of bolts or bolted lap joints when subjected to elevated temperatures. Therefore, this paper aims at studying the effect of loading rates on the strength and deformation capacities of single

shear bolted lap joints and shear tab connections under elevated temperatures. Also, it aims at providing design guidelines that include the effect of loading rate or thermal creep in the bolts when designing shear tab connections for structural fire-engineering applications. Therefore, in this research, two loading rates, 1.5 mm/min (fast) and 0.1 mm/min (slow), are used to test the bolted lap joints under steady-state temperature conditions ranging from 400°C to 700°C with 50°C increment. Then, the rate- and temperature-dependent retention factors for bolt strength capacities are presented and compared with those proposed by previous studies available in the literature. Also, the effect of loading rate and temperature on the bolt pretension force are examined. Then, FE models are developed in ABAQUS (2014) and validated against the experiments performed and previous work available in the literature. These models show the effect of adding the bolts strength reduction coefficient on the capacities and failure modes of shear tab connections at elevated temperatures. Finally, a step-by-step fire design procedure and an example of an isolated shear tab connection are presented. This design illustrates the incorporation of the thermal creep effect in the bolts at elevated temperatures for structural fire-engineering practice.

This investigation is a step forward towards understanding the effect of time on the strength capacities and failure modes of structural bolts and bolted connections at elevated temperatures.

CHAPTER II

THERMAL CREEP BEHAVIOR OF BOLTS

Thermal creep is defined as the time- or rate-dependent behavior of structural steel material that depends on the steel mechanical properties, the applied stress, temperature, and the duration of time. Creep strains become noteworthy when temperatures exceed one-third of the steel melting point, which is around 400°C (Kodur and Dwaikat 2010). The thermal creep of steel can be divided into two categories: explicit and implicit creep. In explicit creep, the material is subjected to constant stress and temperature for a varying period. In this case, the creep strains are added into the strain profile of the cross section of the material (Torić et al. 2013). Then, a creep strain vs. time relationship can be plotted as shown in Fig. 1.

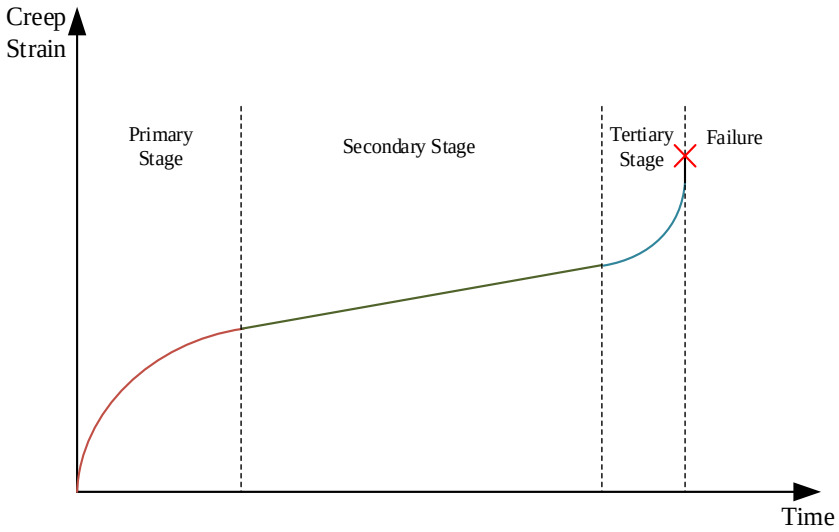

Figure. 1. Stages of thermal creep in steel materials

In the primary stage of creep, the creep strain rate decreases with time due to work hardening phenomena. Then, during the secondary stage, the creep strain rate increases slowly at a constant rate due to the balance between thermal softening and

work hardening. Finally, in the tertiary stage, the creep strain rate increases rapidly due to necking phenomena until failure occurs.

In implicit creep, the material is subjected to varying load, temperature, or both. In this case, creep strains are directly added to the stress-strain curve of the material, as shown in Fig. 2.

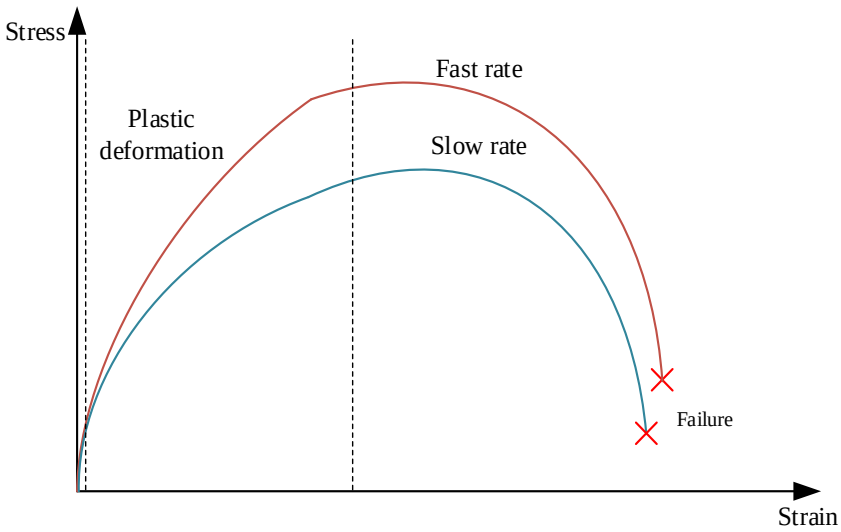

Figure. 2. Effect of loading rate on Stress-Strain curve

Creep strains become noticeable during the plastic deformation phase of the stress-strain curve. In other words, applying a load with a slower rate causes extra strains to occur at each stress level, and a reduction in the ultimate capacity before failure occurs.

Previous studies were performed to show the significance of inelastic creep strains explicitly for bolts at high temperatures (Matar 2014). Tensile creep tests were conducted on A325 bolts at 450°C, 500°C, and 550°C that showed the importance of creep strains when the bolt is subjected to temperatures higher than 400°C. Also, the results indicated that the creep strain rate of the bolt material increases as temperature increases leading to larger creep deformations for higher temperatures.

Therefore, in this study, the investigation of the implicit creep behavior of a single shear-bolted lap joint is detected by varying the loading rate under different elevated temperatures ranging from 400°C to 700°C with 50°C increments.

CHAPTER III

EXPERIMENTAL PROGRAM OF SINGLE SHEAR-BOLTED LAP JOINTS

A. Experimental Program

1. Test Specimens

An experimental program is performed on single shear-bolted lap joints to measure the axial force-displacement relationship at each temperature and loading rate. The lap joints are designed as per AISC 360 *Specifications* (2016) such that the bolt shear failure governs the behavior of the specimen at ambient and elevated temperatures. That is, strength retention factors available in the AISC 360 *Appendix 4* (2016) for the steel base materials and bolts are used to calculate the elevated temperatures capacities of the bolted lap joints. Grade 8.8 M20 X-bolt is used to connect the two S355 steel plates (790 mm×80 mm×20 mm), as shown in Figs. 3(a) and 3(b). The bolts are pre-tensioned using a pre-tensioning wrench with a minimum bolt pretension force of 142 kN as per AISC 360 *Specifications* (2016) for all tests.

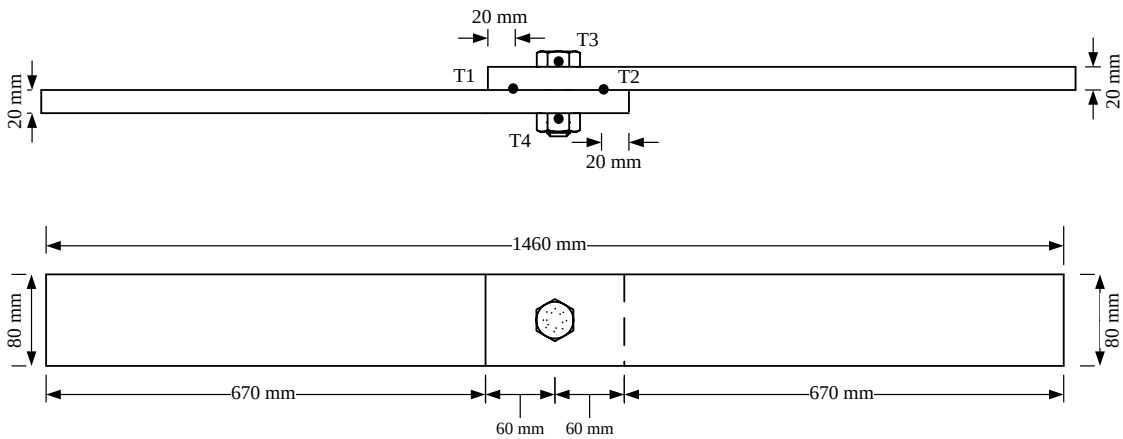

(a)

(b)

Figure. 3. Bolted lap joint specimen: (a) Layout and thermocouples position, (b) Elevation and top view

2. Setup and Instrumentation

A Tinius-Olsen Universal Testing Machine present at the American University of Beirut structure laboratory is used in this study for the tensile testing of the bolted lap joints. An 800 mm×550 mm×830 mm electric furnace is used as a heating device for the elevated temperatures tests. The furnace is made up of three separate heating zones that can be controlled by a temperature control system. The bolt is pre-tensioned before placing the four thermocouples of *type K* on the plates, bolt head, and bolt nut to measure their surface temperatures. Then, the surfaces are wrapped by stainless steel foils (SSF) to protect the thermocouples from direct exposure to the thermal radiation emitted by the heating coils of the furnace. Fig. 3 (a) shows the locations of the four thermocouples distributed on the plate surfaces, bolt head, and bolt nut. The thermocouples T1 and T2 distributed on the plate surfaces are placed 20 mm away from the edges of the top and bottom plates, respectively. Fig. 4 shows a picture of the tested specimen wrapped with stainless steel foils.

Figure. 4. Bolted lap joint wrapped in stainless steel foils

Insulation material is used all around the furnace to prevent heat loss, as shown in Fig. 5. Figure 5 shows the temperature control system used to adjust the temperature inside the furnace, the testing machine, grips, and the thermocouples connected to the data acquisition system. Finally, neither an elevated temperature extensometer nor a camera was used inside the furnace during the tests.

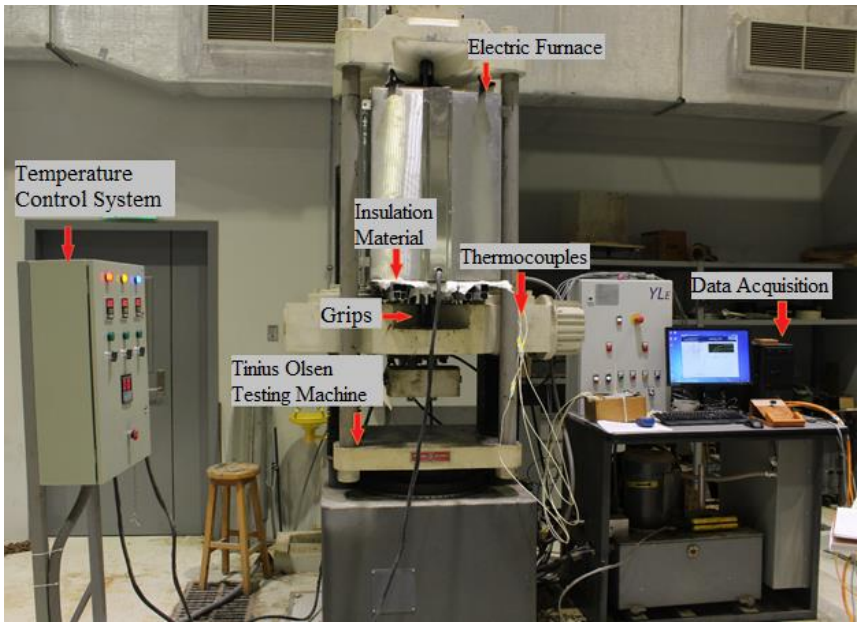

Figure. 5. Experimental Setup

3. Test Loading Protocol

To investigate the effect of loading rates or implicit creep on the behavior of the bolted lap joint specimens, a steady-state temperature analysis is used in this study, rather than a transient analysis. A uniform distribution of high temperature is required to perform a steady-state temperature test. The test loading protocol used is comprised of two phases. In the first phase, the specimen is heated up to a specific temperature and held constant for 30 minutes once the four thermocouples read the same desired temperature to ensure a uniform distribution of temperature along the specimen. The second phase is the loading phase, where a displacement-controlled load is applied to the test specimen with two different rates: fast (1.5 mm/min) and slow (0.1 mm/min). The deformations recorded by the data acquisition system are measured through the crossheads of the Tinius-Olsen Universal Testing Machine. The two loading rates used are chosen arbitrary with a factor of 15 (0.1 mm/min and 1.5 mm/min) to examine the effect of implicit creep on the bolted lap joints strength capacities and deformations. The tests are stopped once the applied force reading is almost null.

B. Test Results

1. Experimental Observation

To investigate the effect of two loading rates on single shear-bolted connections exposed to fire temperature, an experimental program is performed. The results show that all specimens failed in bolt shear fracture at ambient and all elevated temperatures, as shown in Fig. 6.

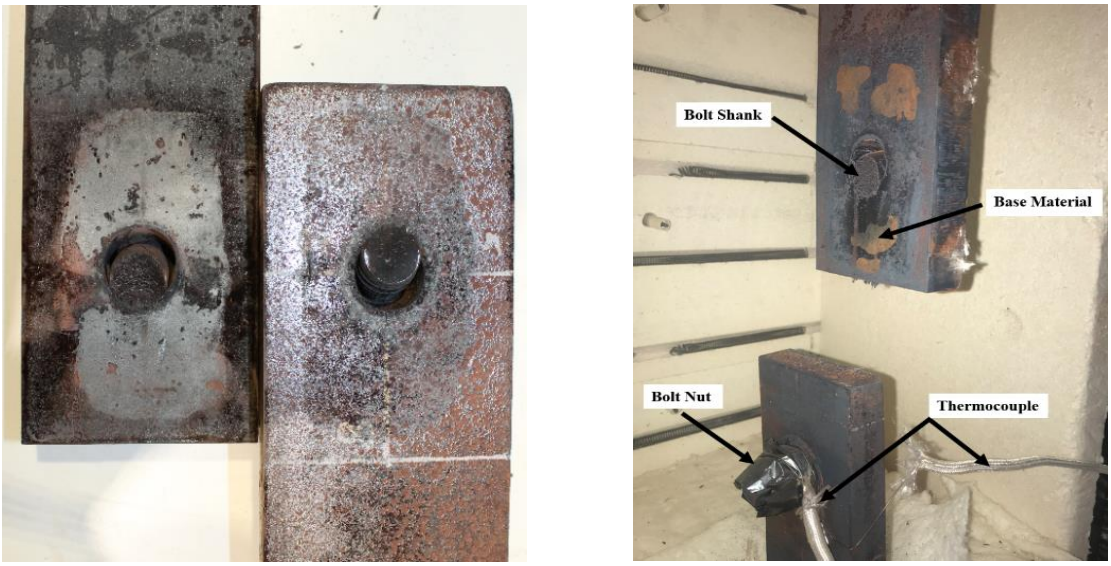

Figure. 6. Bolted lap joints after failure at: (a) 650°C-Slow, (b) 700°C-Slow

Figs. 7 and 8 show the different bolt shear fracture surfaces under all temperatures with the two loading rates. Figs. 7(a) and 8(a) are pictures showing the bolt fracture surface at ambient temperatures using fast and slow loading rates, respectively. The failure mode at ambient temperature is brittle bolt shear failure in both loading rates showing smooth, gray, and shiny surfaces. However, as the temperature increases to 600°C, 650°C, and 700°C, the bolts display a red-brown color with rough surface texture exhibiting a significant ductile failure. Also, for temperatures ranging from 400°C to 550°C, the failure surfaces of both loading rates show a combination of both textures with a visible gray-brown color displaying less ductility. Also, a pop sound is noted at fracture for temperatures less than or equal to 450°C. This indicates that the governing bolt shear failure changes from brittle to ductile at temperatures around 500°C.

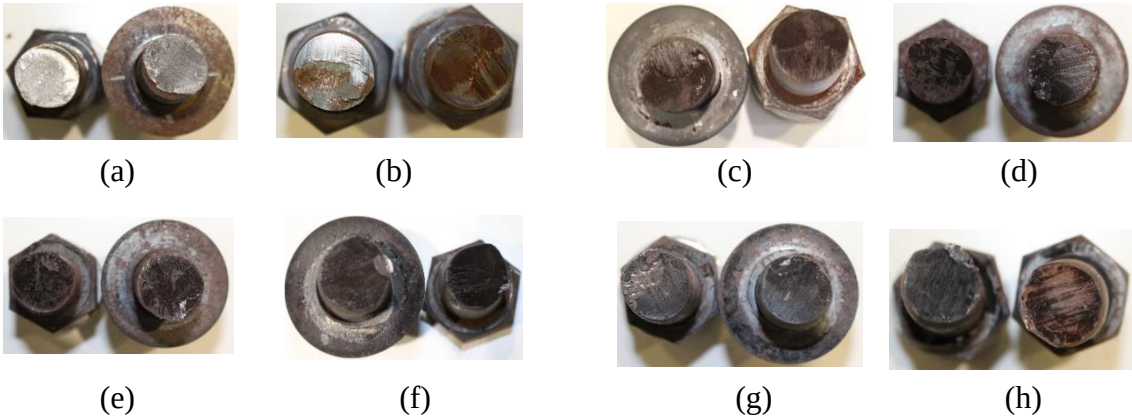

Figure. 7. Bolt fracture surfaces in fast tests at: (a) 20°C, (b) 400°C, (c) 450°C, (d) 500°C, (e) 550°C, (f) 600°C, (g) 650°C, (h) 700°C

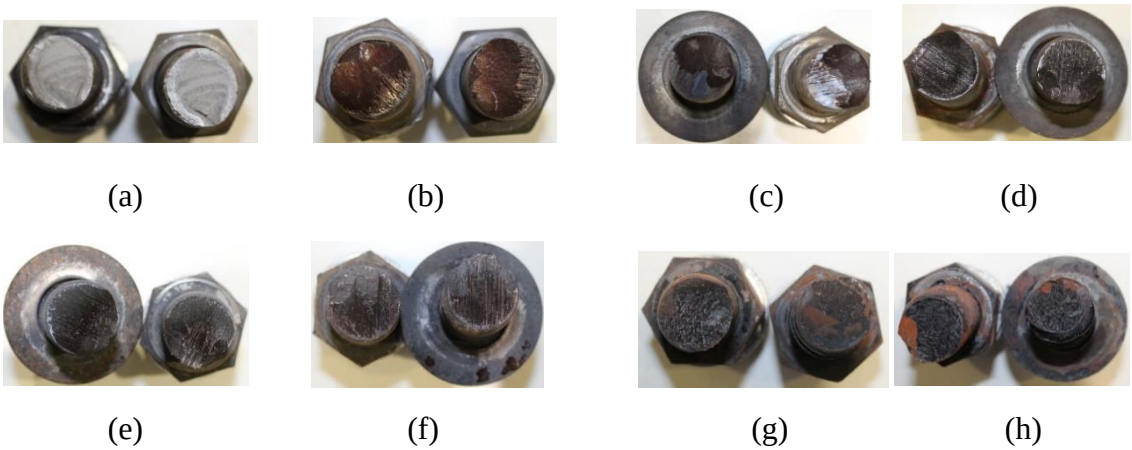

Figure. 8. Bolt fracture surfaces in slow tests at: (a) 20°C, (b) 400°C, (c) 450°C, (d) 500°C, (e) 550°C, (f) 600°C, (g) 650°C, (h) 700°C

Figs. 9 and 10 are pictures of the plate bolt holes after bolt shear failure. It is noted from these figures that the bolts at temperatures larger than or equal to 550°C, using both loading rates, remain attached to the plate bolt hole after fracture occurred. Limited hole ovalization is observed under all temperatures and using both loading rates, indicating no change in failure mode.

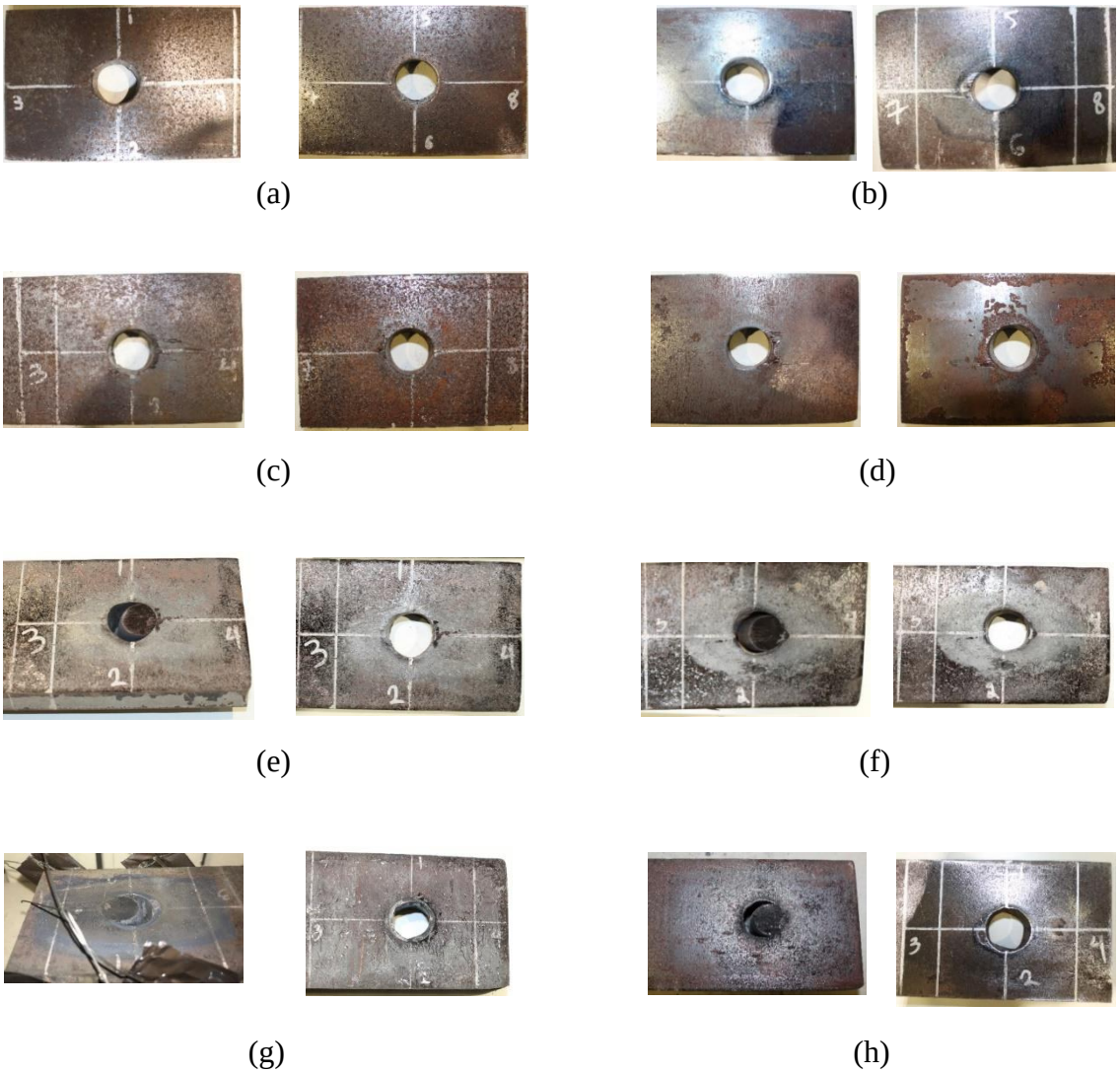

Figure. 9. Bolt holes in fast tests at: (a) 20°C, (b) 400°C, (c) 450°C, (d) 500°C, (e) 550°C, (f) 600°C, (g) 650°C, (h) 700°C

(e) (f)

(g) (h)

Figure. 10. Bolt holes in slow tests at: (a) 20°C, (b) 400°C, (c) 450°C, (d) 500°C, (e) 550°C, (f) 600°C, (g) 650°C, (h) 700°C

2. Temperature-Dependent Behavior

a. Effect of Temperature on Load-Deformation Relationship

To study the temperature-dependent behavior of the Grade 8.8 bolt, the results from the tensile testing of the single shear-bolted lap joints at different elevated temperatures with both loading rates are presented in Figs. 11(a) and 11(b). Initially, the curve increases linearly, representing the initial stiffness of the bolted lap joint at a targeted temperature. As temperature increases, initial stiffness starts to degrade. It can be noticed that the capacity of the lap joint connection decreases when temperature increases and drops further when the slower loading rate is applied. Table 1 presents the peak loads (P) and the maximum connection displacements (Δ) for all tested specimens under different temperatures and loading rates. Fig. 11 shows a sharp drop in the bolt strength capacities at temperatures between 20°C and 400°C and 400°C and 500°C for both loading rates. More specifically, at 400°C, the bolt strength is reduced by 42% and 39% of its initial strength capacity at ambient temperature for both fast and

slow loading tests, respectively. As temperature increases up to 700°C, the reduction of the bolt strength reaches its maximum of 89% and 92% for fast and slow tests, respectively. Further, the increase in axial displacement as temperature increases indicates that the lap joint behaves in a more ductile manner in fire events. For instance, the maximum axial displacement at 400°C-*Fast* is equal to 21.3 mm and increases till it reaches 48.3 mm at 700°C-*Fast*, as shown in Table 1. Also, Table 1 shows that the maximum axial displacement increases in the slow rate tests from 24.5 mm at 400°C-*Slow* to 38.5 mm at 700°C-*Slow*.

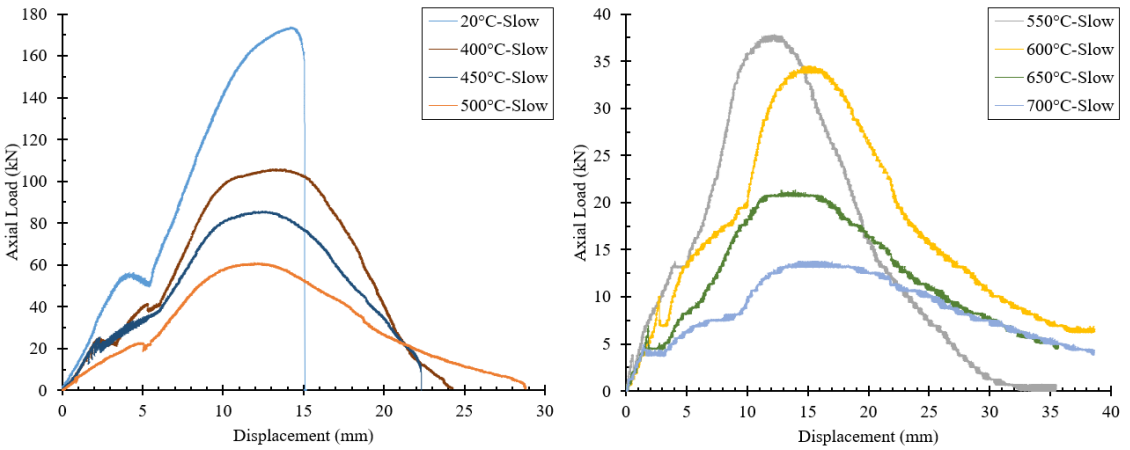

(a)

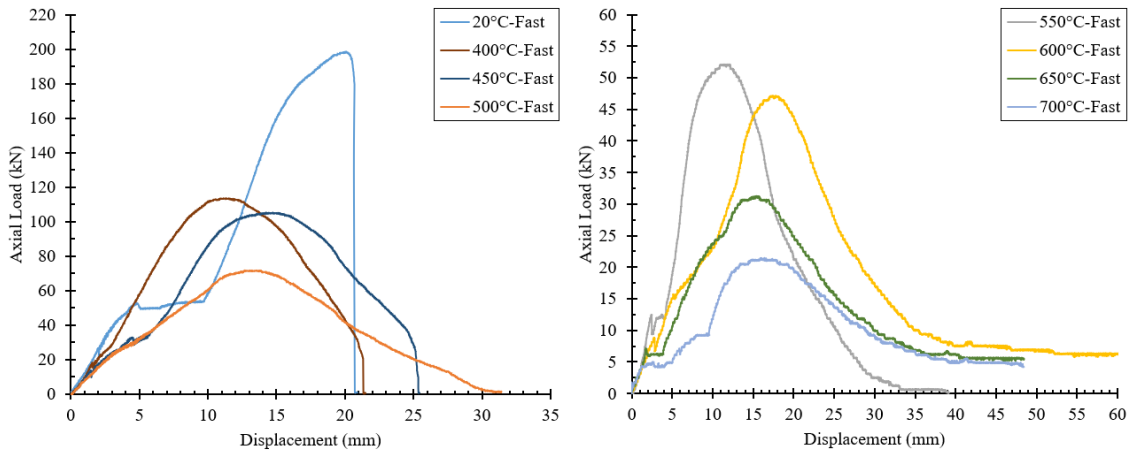

(b)

Figure. 11. Force-displacement results for: (a) Fast loading rate, (b) Slow loading rate

Table. 1. Test matrix and results of failure load and displacement for fast and slow rate

Test Name	Temperature (°C)	Peak Load, P (kN)	Failure Axial Displacement, Δ (mm)
20°C-Fast	20	198.4	20.1
400°C-Fast	400	113.8	21.3
450°C-Fast	450	104.5	25.7
500°C-Fast	500	71.4	31.4
550°C-Fast	550	52.1	39.1
600°C-Fast	600	47.1	60.0
650°C-Fast	650	31.2	48.3
700°C-Fast	700	21.4	48.3
20°C-Slow	20	173.3	15.2
400°C-Slow	400	105.5	24.5
450°C-Slow	450	85.5	22.4
500°C-Slow	500	60.6	28.8
550°C-Slow	550	37.8	32.2
600°C-Slow	600	34.4	36.6
650°C-Slow	650	21.3	35.6
700°C-Slow	700	13.7	38.5

b. Effect of Temperature on Bolt Pretension Force

In a slip-critical connection, the pretension forces cause the connected plates to be clamped together, producing friction forces that resist the applied shear loads (Guo et al. 2017). When the applied load reaches the slip-critical capacity of the bolt, slip occurs. Slippage in the performed experiments is shown in two different phenomena, either as a constant or gradual slip. As shown in Fig. 11, tests at 20°C-*Fast*, 550°C-*Fast*, and 650°C-*Fast* show that constant slip occurs at forces around 52kN, 12kN, and 6kN, respectively. However, for the other tests, slip occurs gradually within a range referred to as lower and upper bounds. Table 2 shows the lower and upper bounds of pretension forces resulting from all tests conducted in this study. The retention factors are calculated by dividing the lower bound of the pretension force at each temperature to that at ambient temperature for each corresponding loading rate. The results show that there is no major difference in the bolt pretension forces when both loading rates

are used. Thus, the retention factors presented are the average between those obtained from the tests conducted using fast and slow rates. Fig. 12 presents the temperature-dependent retention factors for minimum bolt pretension forces of Grade 8.8 M20 X-bolts and the corresponding proposed equation using linear regression analysis. The variation of retention factors for pretension force, k_{PT} , as a function of temperature, T, is shown in Eq. (1) with a coefficient of determination: $R^2 \simeq 0.99$:

$$k_{PT} = -0.0009T + 0.692 \tag{1}$$

Eq. (1) is only valid for temperatures ranging from 400°C to 700°C. These retention factors can be used in the slip-resistance design equation (J3-4) available in the AISC 360 *Specifications* (2016) to predict elevated temperatures slip-critical capacities.

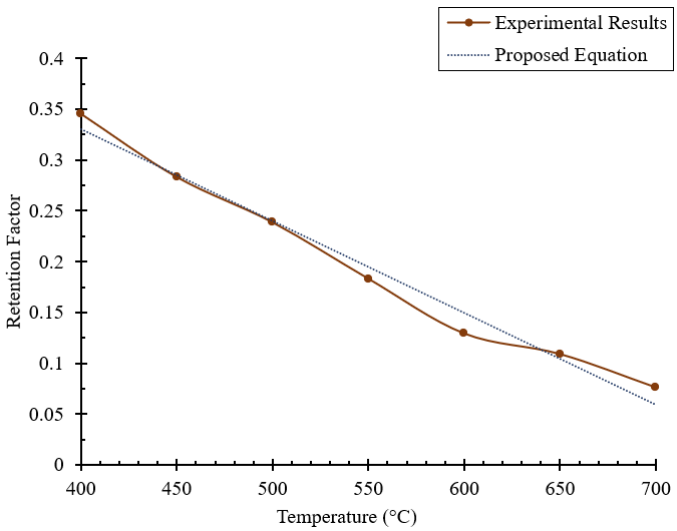

Figure. 12. Retention factors for minimum bolt pretension force of Grade 8.8 M20 bolt

Table. 2. Lower and upper bound pretension force

Test Name	Lower Bound Pretention Force (kN)	Upper Bound Pretention Force (kN)	Test Name	Lower Bound Pretention Force (kN)	Upper Bound Pretention Force (kN)
20°C-Fast	49.5	53.6	20°C-Slow	56.1	53.1
400°C-Fast	15.4	27.2	400°C-Slow	21.3	40.3
450°C-Fast	13.4	33.3	450°C-Slow	16.6	37.4
500°C-Fast	10.0	20.0	500°C-Slow	15.4	21.7
550°C-Fast	12.4	12.4	550°C-Slow	6.5	13.3
600°C-Fast	6.7	23.1	600°C-Slow	6.9	19.5
650°C-Fast	6.9	6.2	650°C-Slow	4.5	9.5
700°C-Fast	4.2	9.2	700°C-Slow	3.8	8.4

3. Time-Dependent Behavior

a. Effect of Loading Rate on Load-Deformation Relationship

To study the effect of loading rates on a single-shear bolted lap joint subjected to different elevated temperatures, axial force-displacement curves are illustrated in Figs. 13 and 14. Figs. 13 and 14 show a comparison between the bolted lap joint behavior obtained at temperatures ranging between 20°C to 500°C and 550°C to 700°C, respectively, under both loading rates. It can be noted that the difference in capacities at ambient temperatures for both loading rates, as shown in Fig. 13 (a), might be due to the different material strength, dimension tolerance, and hole diameter. However, at 400°C (Fig. 13(b)), there is no major effect when using a slower loading rate on the strength capacity of the bolted lap joint. As temperature increases up to 450°C and 500°C, the difference in strength capacities becomes noticeable as shown in Figs. 13(c) and 13 (d), respectively. This is since creep has no significant effect at temperatures below one-third of the melting point of steel (400°C) (Kodur and Dwaikat 2010).

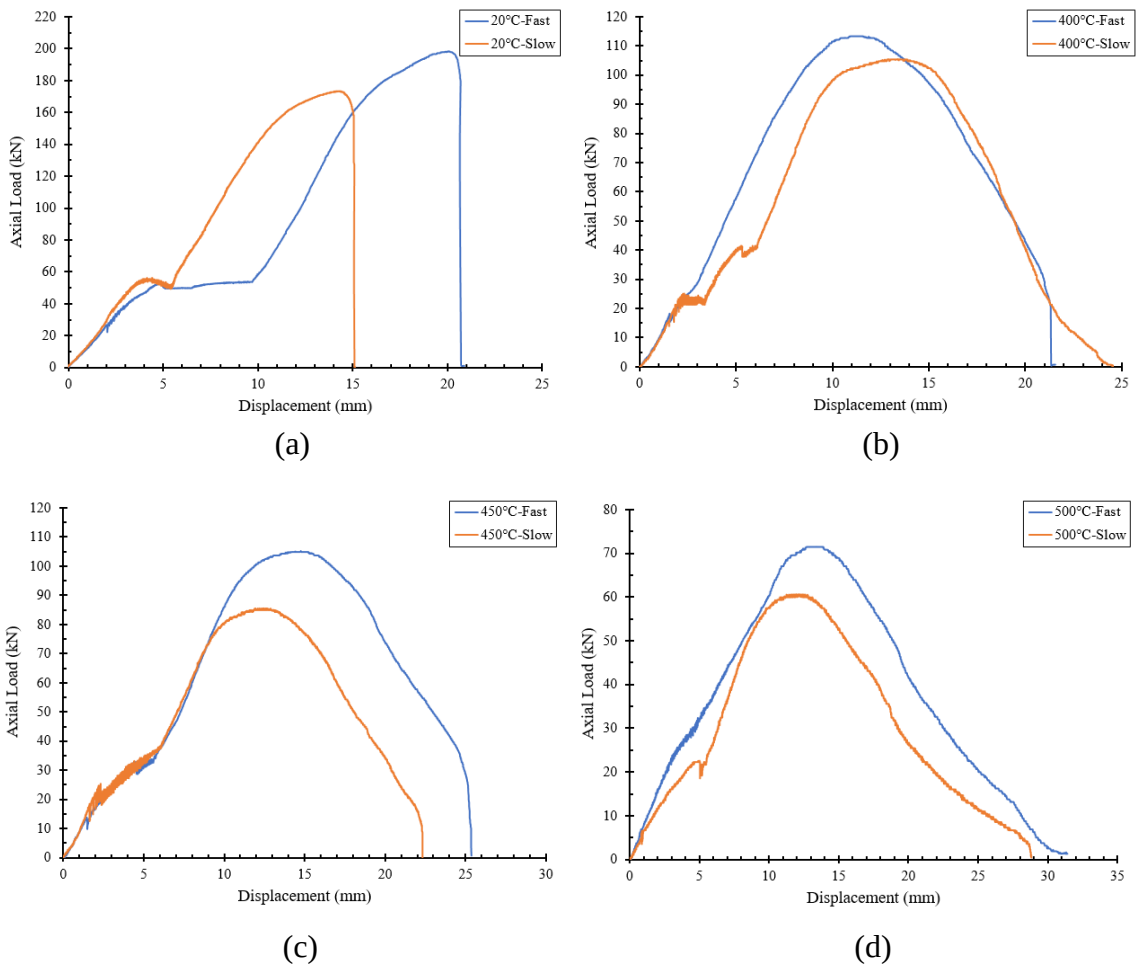

Figure. 13. Effect of loading rate on force-displacement behavior at: (a) 20°C, (b) 400°C, (c) 450°C, (d) 500°C

As temperature increases, the difference in bolt strength capacities starts to increase more significantly when temperatures reach 550°C, 600°C, and 650°C as shown in Figs. 14(a), 14(b), and 14(c), respectively. The difference in strength capacities continues to increase until it reaches its maximum at 700°C with values of 21.4 kN and 13.7 kN using fast and slow rates, respectively, as shown in Fig. 14 (d). Table 3 presents the percentage decrease in bolt shear capacities for the bolted lap joints when subjected to both loading rates. As tabulated in Table 3, the percentage decrease in capacities when a slower loading rate is used shows a major effect at temperatures above 450°C. That is, the bolt shear capacity decreases by 18% at 450°C

until it reaches its maximum value of 36% decrease at 700°C. This reduction occurs due to the significant inelastic creep strains that initiate at temperatures slightly above the recrystallization temperature of steel (Boresi and Schmidt 1993). The results also show no major rate-dependent effect on neither the pretension force nor the initial stiffness, indicating that the inelastic creep strains are not significant for low stress or load levels. Figs. 14(c) and 14(d) show the force-displacement relationships for tests conducted at 650°C and 700°C, respectively, using fast and slow loading rates. It can be clearly observed that the bolt shear capacity at 650°C-*Slow* and 700°C-*Fast* give the same value of 21 kN. Therefore, ignoring the rate-dependent behavior of bolts in the fire design of steel bolted connections can result in unsafe predictions.

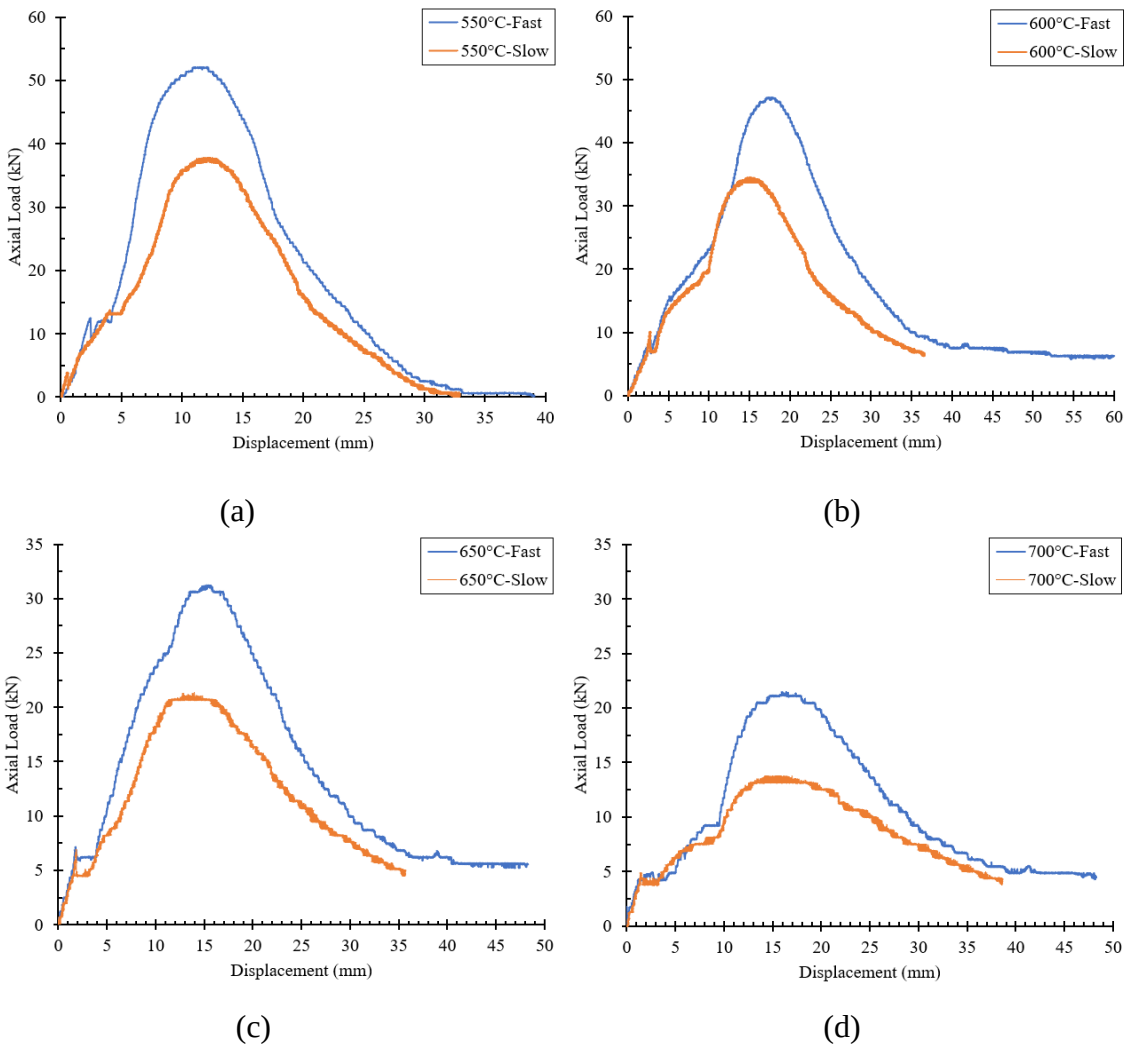

Figure. 14. Effect of loading rate on force-displacement behavior at: (a) 550°C, (b) 600°C, (c) 650°C, (d) 700°C

Table. 3. Effect of loading rate on the strength capacities of the single shear-bolted lap joints

Test Name	Failure Load, P (kN)	Test Name	Failure Load, P (kN)	Decrease in Capacity (%)
20°C-Fast	198.4	20°C-Slow	173.3	12.3
400°C-Fast	113.8	400°C-Slow	105.5	7.3
450°C-Fast	104.5	450°C-Slow	85.5	18.0
500°C-Fast	71.4	500°C-Slow	60.6	14.7
550°C-Fast	52.1	550°C-Slow	37.8	27.4
600°C-Fast	47.1	600°C-Slow	34.4	27.0
650°C-Fast	31.2	650°C-Slow	21.3	31.7
700°C-Fast	21.4	700°C-Slow	13.7	36.0

b. Retention Factors

The retention factors for the two loading rates are presented for the Grade 8.8 bolt subjected to single shear. The retention factors for the bolt shear capacity is calculated by dividing the capacities at each designated temperature by that at ambient temperature. The bolt shear capacity at each elevated temperature in both loading rates are divided by the average capacity of both rates at ambient that is equal to 185.9 kN. Fig. 15 shows a comparison between the retention factors from this study against those by AISC 360 *Appendix 4* (2016), Yang et al. (2011), Kodur et al. (2012), and Fischer et al. (2017). The results show a significant effect of the loading rate on the retention factors of bolt shear strength capacity for temperatures beyond 450°C. This indicates that more conservative retention factors are obtained from the slow loading rate tests than those resulting from the fast tests and all other previous studies. Also, the retention factors obtained from the fast tests at temperatures up to 600°C are more conservative than those proposed by previous studies. However, beyond 600°C, these retention factors, as well as those available in the literature, show a close match. This shows that neglecting the effect of loading rates might lead to unsafe and inaccurate results in

predicting the bolt shear capacity in bolted connections when exposed to elevated temperatures.

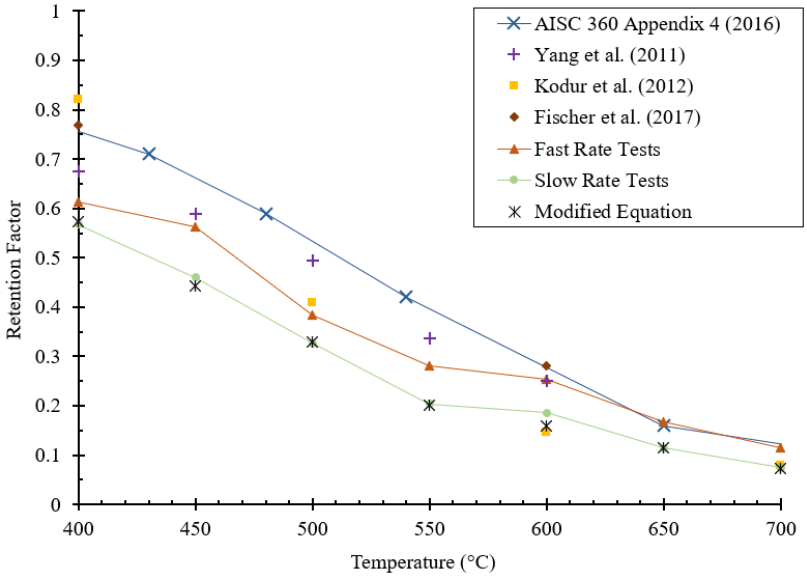

Figure. 15. Proposed bolt shear capacities retention factors in comparison with previous data and modified equation

c. <u>Proposed Retention Factors Modification</u>

To include the effect of creep implicitly in the design of bolted connections at elevated temperatures, a strength reduction coefficient, α, is proposed and added to the bolt shear capacity equation (J3-1) available in the AISC 360 *Specifications* (2016), as shown in Eq. (2):

$$R_v = \alpha K_{bt} A_b F_{nv} \tag{2}$$

The strength reduction coefficient, α, is defined as the ratio of the slow rate retention factors (from tests) to the AISC 360 retention factors available in *Appendix 4* (2016). For temperatures ranging from 400°C to 600°C, a linear regression analysis is performed to find a relationship between, α, and temperature, T, with a coefficient of determination: $R^2 \simeq 0.98$, as shown in Eq. (3):

$$\alpha = -0.0014T + 1.3 \tag{3}$$

For temperatures larger than 600°C, the value of α no longer applies for the linear relationship proposed in Eq. (3). The strength reduction coefficients (α) at temperatures 600°C, 650°C, and 700°C are found to be 0.84, 0.72, and 0.74, respectively. Therefore, the conservative value of α for temperatures larger than 600°C is considered 0.72. Fig. 15 shows the retention factors of the modified AISC 360 (2016) equation (Eq. (2)) against those available in the literature (AISC 360 *Appendix 4* (2016), Yang et al. (2011), Kodur et al. (2012), and Fischer et al. (2018)). This proposed strength reduction coefficient, α, produces more conservative bolt shear strength capacities at elevated temperatures when including the effect of implicit creep or loading rate.

CHAPTER IV

FINITE ELEMENT MODELS

A. Finite Element Modelling

In this research, the finite element package ABAQUS (2014) is used to reproduce the experimental program performed and shear tab connections available in the literature at elevated temperatures (Yu et al. 2009; Hu and Engelhardt 2012; Fischer et al. 2018). The aim of these models is to predict the effect of thermal creep on the behavior, strength capacities, and failure modes of simple bolted connections at temperatures larger than 400°C.

1. Model Discretization

The models are integrated using eight-node three-dimensional solid elements. In the regions where the failure is most likely to occur, such as the bolt shank and the beam web, a finer mesh of 0.1 mm is used to help predict accurate results. A surface-to-surface contact with a finite sliding interaction is used to replicate the contact surfaces between all of the components. The finite sliding formulation is used to allow for separation, sliding, and rotation of the surfaces in contact. A friction coefficient of 0.25 is used.

2. Material Properties

A bilinear model is used to input the mechanical properties of the steel materials. To predict the steel material properties at elevated temperatures, retention factors proposed by AISC 360 *Appendix 4* (2016) are used for the base materials. However, for the Grade 8.8 bolts material, retention factors proposed by Kodur et al. (2012) are used. In this experimental program, material properties of S355 for the base

material and Grade 8.8 for the bolts are inputted. For Yu et al. (2009) the column material was S355, the beam and shear tab S275, and 3 Grade 8.8 bolts were used. For Hu and Engelhardt (2012), the base plates and beam material were S355, the shear tab connection was S275. For Fischer et al. (2018), the base material was S275 connected by one Grade 8.8 bolt. *Poisson*'s ratio is equal to 0.3 constant at all temperatures.

3. Geometry and Boundary Conditions

All models are reproduced using ABAQUS (2014). The models are loaded in two steps. In the first step, where applicable, the bolts are pre-tensioned by applying a pressure on the bolt head and bolt nut equivalent to the minimum bolt pretension force divided by the surface area. Then, a displacement-controlled load is applied corresponding to the testing procedures. Also, a fixed boundary condition is set during the entire simulations.

B. Finite Element Validations and Results

1. This research Experimental Program

Sixteen single shear bolted lap joints are tested using two different loading rates: fast (1.5 mm/min) and slow (0.1 mm/min) under steady state temperature conditions. The tests using the fast loading rate are first validated using ABAQUS (2014). All the bolted lap joints failed in bolt shear in the simulations as in the experimental results. The mesh of the models, and the bolt shear failure are shown in Figs. 16(a) and 16(b), respectively.

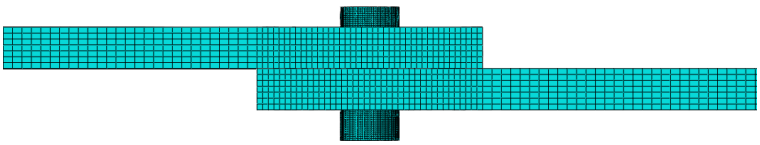

(a)

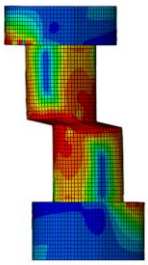

(b)

Figure. 16. FE results for single shear bolted lap joint (a) Mesh, (b) Bolt Failure

The models predict the force-axial displacement relationships with a very high accuracy at temperatures 450°C, 500°C, 550°C, 600°C, 650°C, and 700°C, as shown in Fig. 17. Eq. (1) is adopted to predict the temperature-dependent retention factors for the slip-critical capacities at elevated temperatures, which also shows a very accurate result. After validating the fast tests, Eqs. (2) and (3) are used to incorporate the effect of thermal creep in the Grade 8.8 bolt materials in ABAQUS (2014). After adding the strength reduction coefficient, α , in the bolt strength capacities, the results validate the slow rate force-displacement relationships, as shown in Fig. 17. This proves that neglecting the time-dependent effect or the thermal creep effect of bolt materials at elevated temperatures might result in unsafe and inaccurate predictions of bolted lap joints and shear tab connections strength capacities.

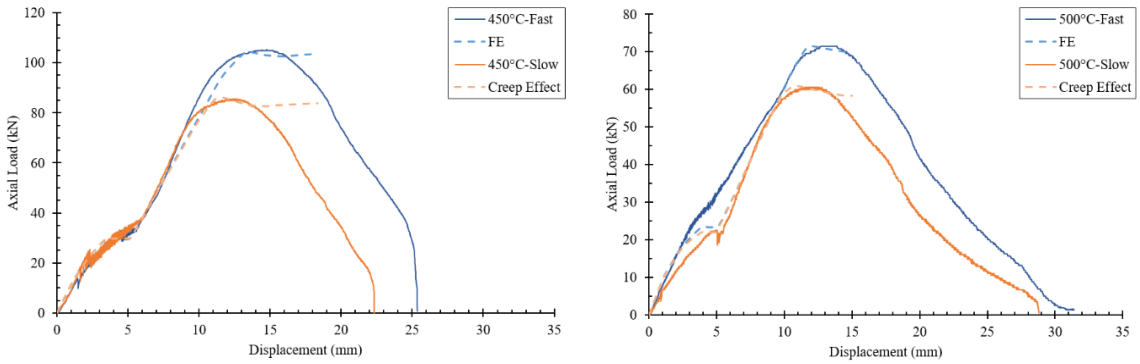

(a) (b)

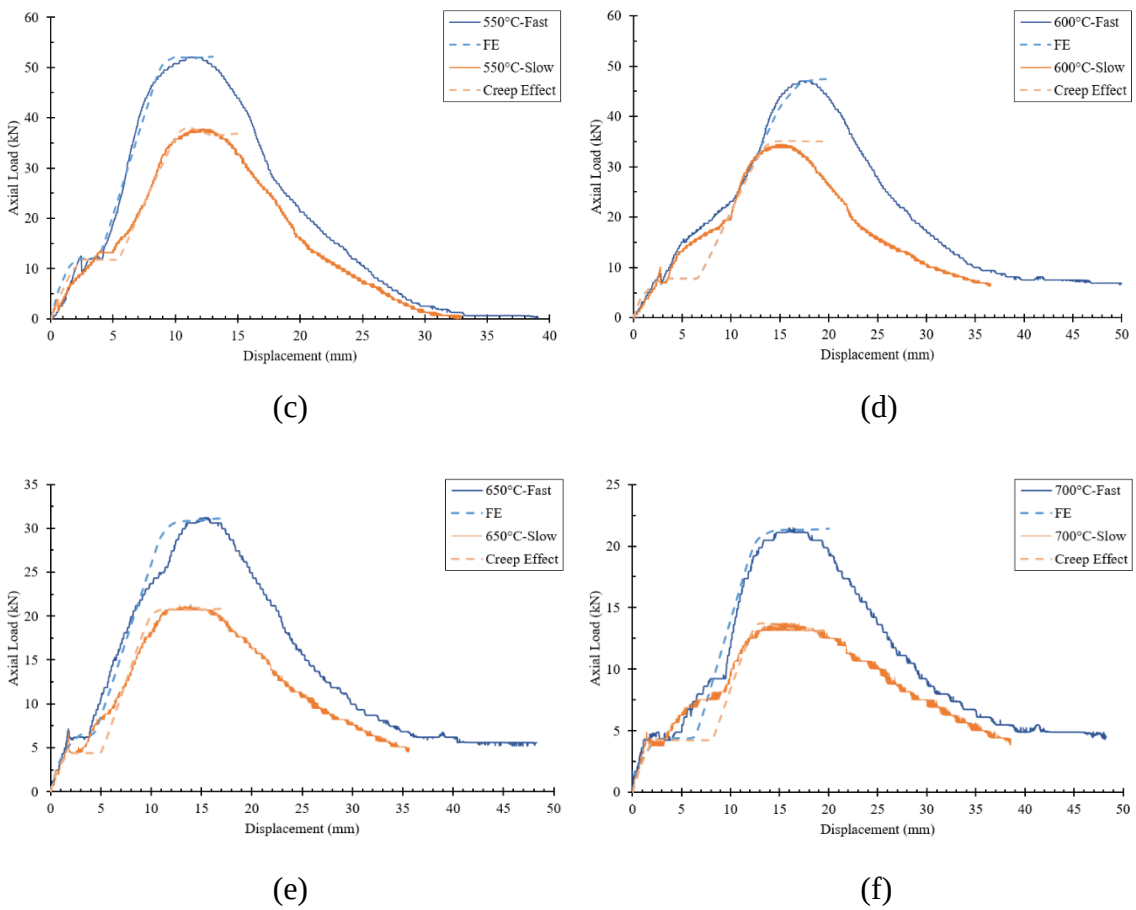

Figure. 17. Load-Displacement Validations and effect of creep at: (a) 450°C, (b) 500°C, (c) 550°C, (d) 600°C, (e) 650°C, (f) 700°C

2. *Yu et al. (2009)*

Three experimental tests performed by Yu et al. (2009) on shear tab connections are simulated. These connections are subjected to inclined loading with 35° inclination at temperatures 450°C, 550°C, and 650°C. Figs. 18(a) and 18(b) show the mesh of the shear tab connections and the results after loading, respectively. Figs. 19(a), 19(b), and 19(c) show a comparison between the experimental and FE results of the force-rotation relationships at 450°C, 550°C, and 650°C, respectively. The results show that the FE models predict the experimental results with high accuracy. The temperature-dependent retention factors for the bolt pretension force proposed in Eq. (1) are used to predict the

slip-critical capacities at all temperatures showing a very good accuracy. As shown in Table 4, the ultimate strength capacity of the shear tab connection is 84 kN with 5.6° rotation at 450°C. After incorporating the effect of thermal creep by applying Eqs. (2) and (3) in the Grade 8.8 bolt material in ABAQUS (2014), the strength capacity decreases by 33.1% to reach 56.2 kN, as shown in Table 4 and Fig. 19(a). The connection rotation also decreases to 4.2° at 450°C. The strength capacity continues to degrade until it decreases by 47.1% and 40.1% at temperatures 550°C and 650°C, as shown in Figs. 19(b) and 19(c), respectively. The results of these simulations show that using Eq. (2) gives a more conservative result, as compared to AISC 360 *Specifications* (2016), when predicting the strength capacities and rotations of shear tab connections at temperatures larger than 400°C.

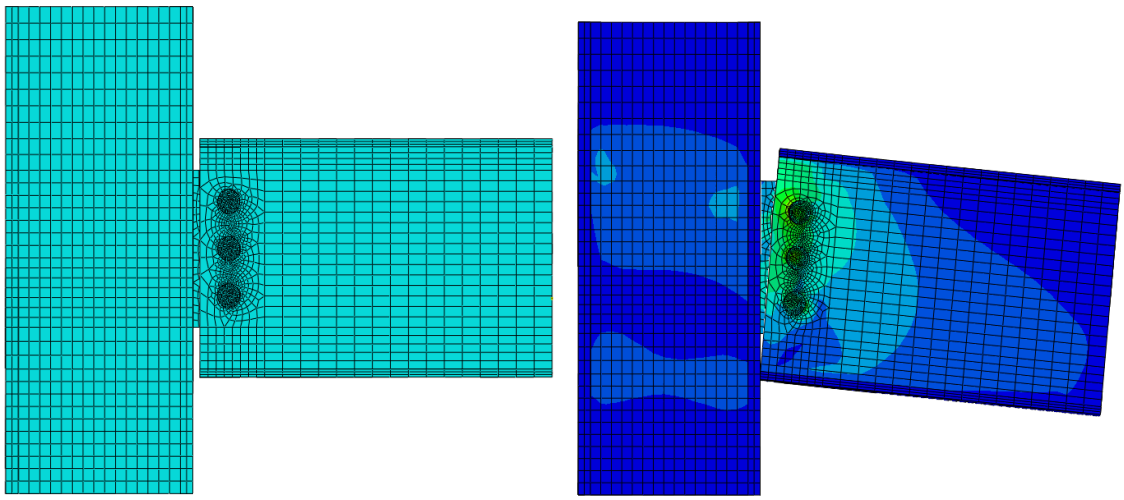

(a) (b)

Figure. 18. FE results for shear tab connection (a) Mesh, (b) Results

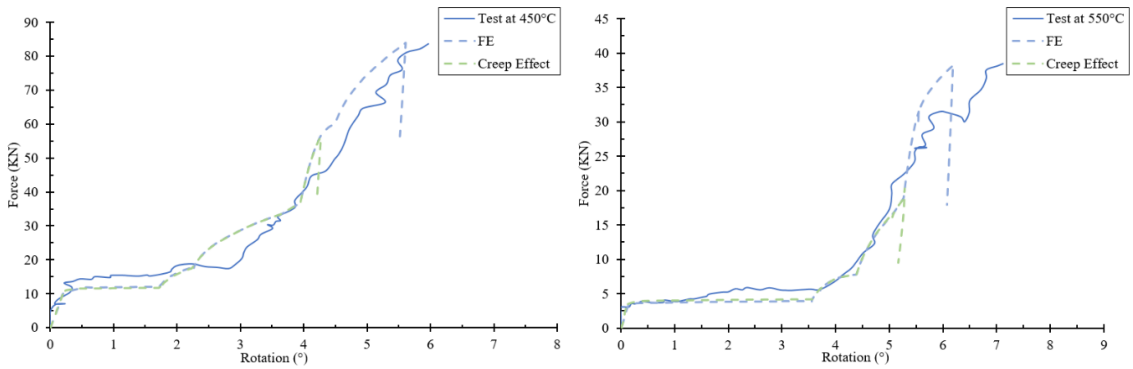

(a) (b)

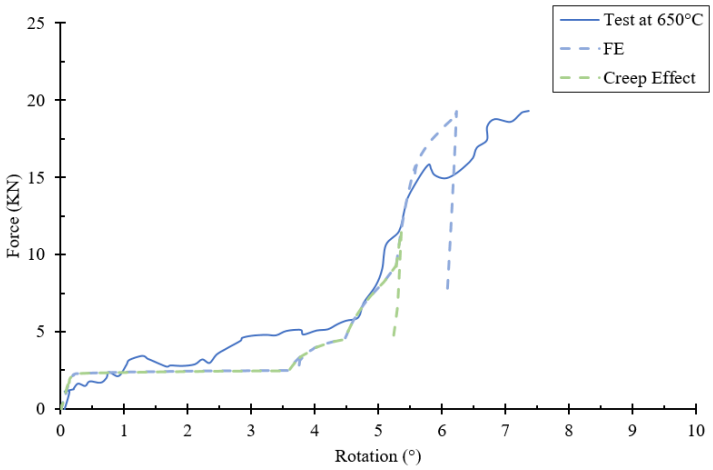

(c)

Figure. 19. Load-Rotation Validations and effect of creep at: (a) 450°C, (b) 550°C, (c) 650°C

Table. 4. FE results for the effect of thermal creep on shear tab connections strength capacity and rotation

Test Temperature	Failure Load, P (kN)	Failure Load, P (kN) (creep effect)	Capacity Decrease (%)	Rotation (°)	Rotation (°) (creep effect)
450°C	84.0	56.2	33.1	5.6	4.2
550°C	38.4	20.3	47.1	6.1	5.2
650°C	19.2	11.5	40.1	6.2	5.3

3. *Hu and Engelhardt (2012)*

Eight experiments performed by Hu and Engelhardt (2012) on single-plate connections (shear tab connections) are simulated using ABAQUS (2014). The experiments are subjected to inclined and axial loading at 500°C and 700°C using M20 and M24 Grade 8.8 bolts. Figs. 20(a), 20(b), 20(c), and 20(d) show the force-displacement and force-rotation validations at 500°C using M20 and M24 bolts. The models predict the curves with a very high accuracy. After adding the effect of thermal creep in the models, the failure mode at 500°C-M20-axial and 500°C-M20-inclined remained bolt shear failure and the ultimate bolt strength capacities decreased by 45.5% and 39.6%, respectively, as shown in Table 5. However, for 500°C-M24-axial and 500°C-M24-inclined, the connection failed in tear-out of the beam web and changed to bolt shear failure after adding the effect of thermal creep to the bolts materials, as shown in Figs. 21(a) and 21(b) and Table 5.

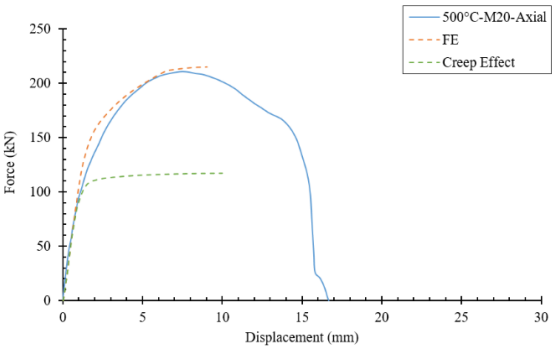

(a)

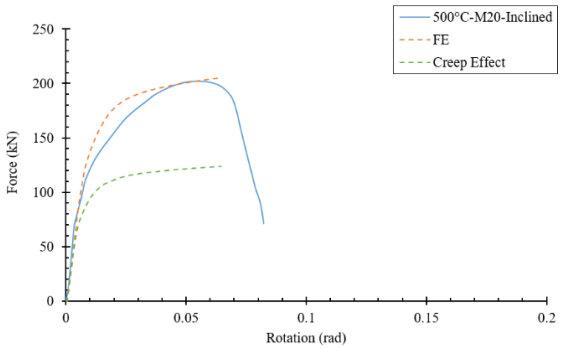

(b)

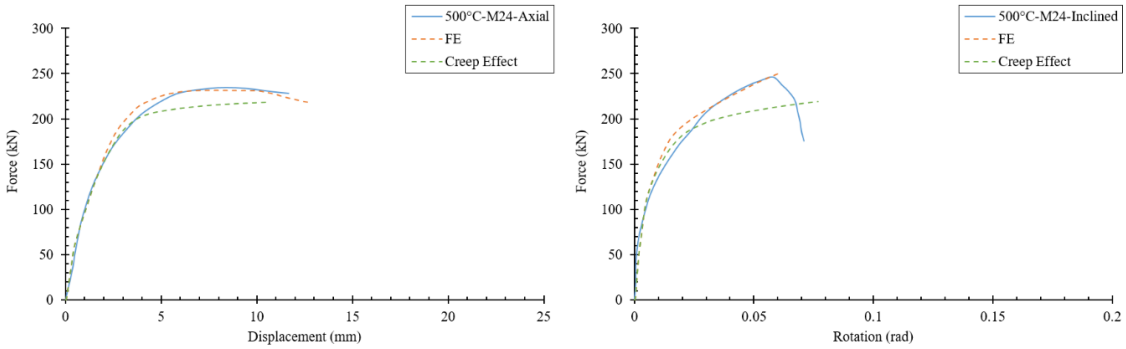

(c) (d)

Figure. 20. Load-Displacement and Load-Rotation Validations and effect of creep at: (a) 500°C-M20-Axial, (b) 500°C-M20-Inclined, (c) 500°C-M24-Axial, (d) 500°C-M24-Inclined

Table. 5. FE results for the effect of thermal creep on shear tab connections strength capacity and failure mode

Test Name	Failure Load, P (kN)	Failure Load, P (kN) (creep effect)	Failure Mode	Failure Mode (creep effect)	Capacity Decrease (%)
500°C-M20-Axial	215.1	117.1	Bolt Shear	Bolt Shear	45.5
500°C-M20-Inclined	205.1	123.7	Bolt Shear	Bolt Shear	39.6
500°C-M24-Axial	231.4	218.3	Tear-out	Bolt Shear	-
500°C-M24-Inclined	251.7	219.1	Tear-out	Bolt Shear	-
700°C-M20-Axial	47.5	23.7	Bolt Shear	Bolt Shear	50.1
700°C-M20-Inclined	47.7	35.0	Bolt Shear	Bolt Shear	26.6
700°C-M24-Axial	68.3	44.6	Tear-out	Bolt Shear	-
700°C-M24-Inclined	69.0	52.1	Block Shear	Bolt Shear	-

Figs. 22(a), 22(b), 22(c), and 22(d) show the force-displacement and force-rotation validations at 700°C using M20 and M24 bolts. The results of the FE simulations show a high accuracy in predicting the experimental results. At 700°C-M20-axial and 700°C-M20-inclined, the shear tab connection failed in bolt shear before and after adding the effect of thermal creep to the bolts materials, with a decrease in capacity by 50.1% and 26.6%, respectively. Also, after adding the effect of thermal creep, the failure mode changed from tear-out and block shear of the beam web to bolt shear failure at 700°C-M24-axial and 700°C-M24-inclined, respectively, as shown in

Figs. 23(a), 23(b), 23(c), and 23(d), and Table 5. This shows that neglecting the effect of time or creep when designing shear tab connections in fire results in unsafe predictions of both the failure mode and the ultimate strength capacities.

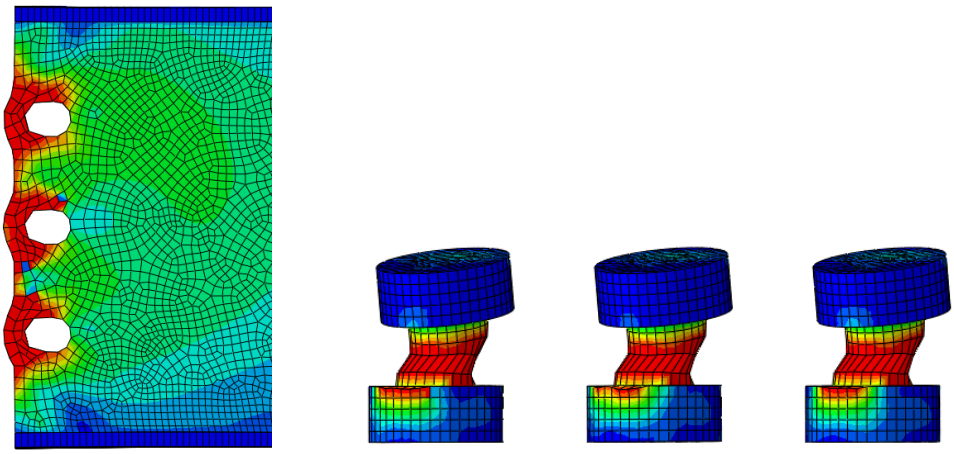

(a) (b)

Figure. 21. FE Results at 500°C-M24-axial: (a) Beam web tear-out before creep effect, (b) bolt shear failure after creep effect

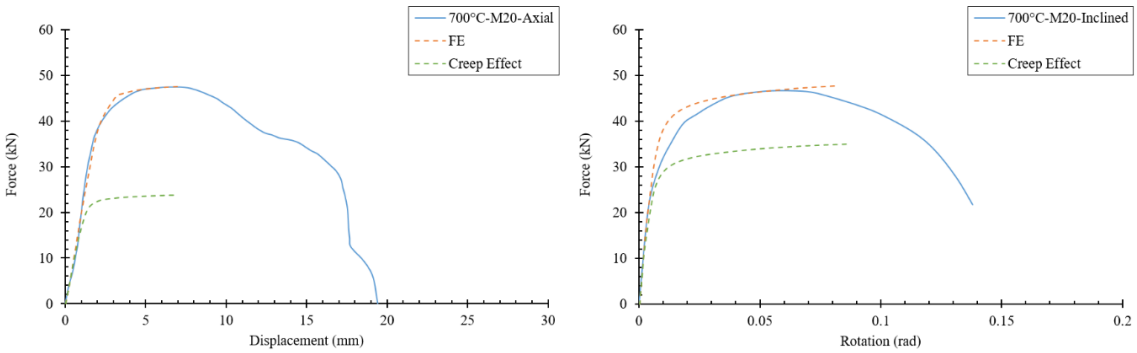

(a) (b)

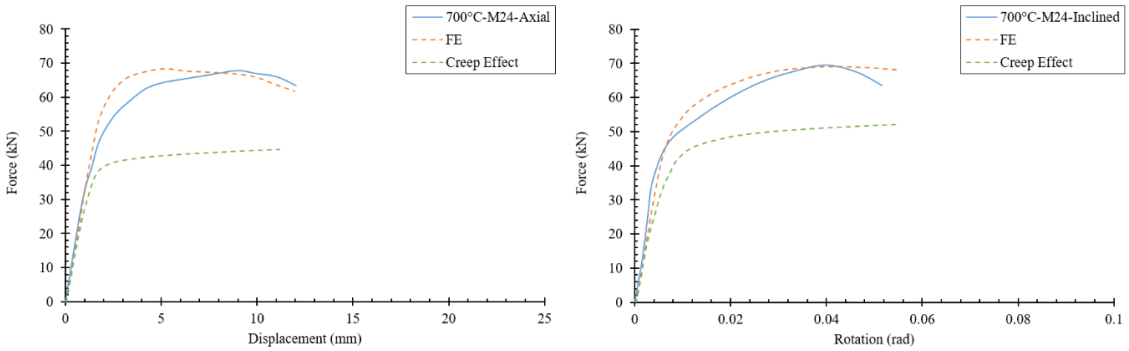

(c) (d)

Figure. 22. Load-Displacement and Load-Rotation Validations and effect of creep at: (a) 700°C-M20-Axial, (b) 700°C-M20-Inclined, (c) 700°C-M24-Axial, (d) 700°C-M24-Inclined

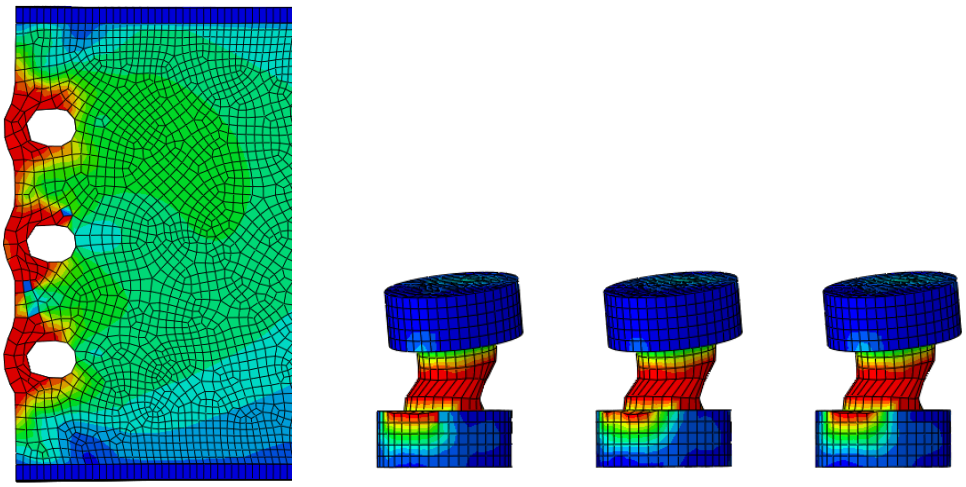

(a) (b)

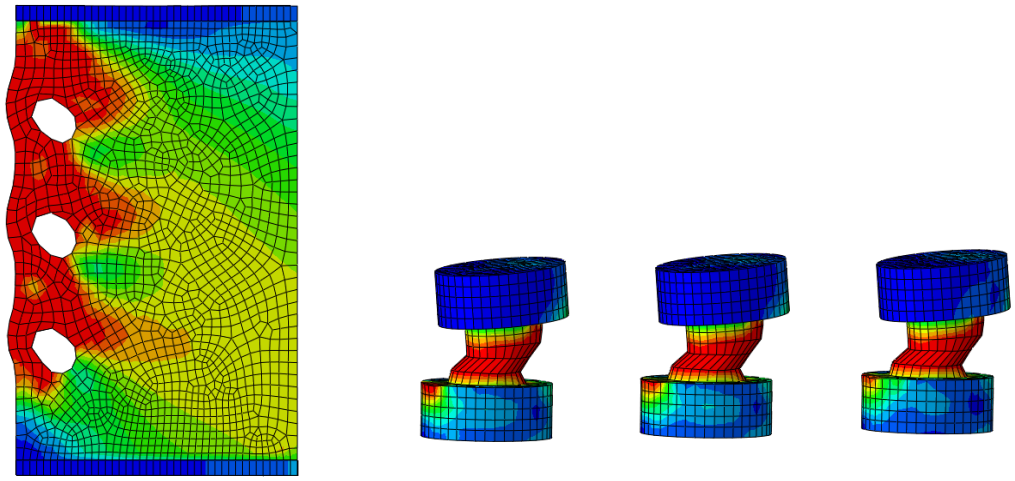

(c) (d)

Figure. 23. FE Results at 700°C-M24-axial: (a) Beam web tear-out before creep effect, (b) bolt shear failure after creep effect, and at 700°C-M24-inclined: (c) Beam web block shear before creep effect, (d) bolt shear failure after creep effect

4. Fischer et al. (2018)

Three experimental tests performed on single-bolted lap joints (LJ-1, LJ-2, and LJ-3) were also simulated, which are simple representations of shear tab connections (Fischer et al. 2018). The lap joints are all performed at 600°C and using different configurations, as shown in Table 6. Figs. 24(a), 24(b), and 24(c) show the force-displacement relationships of the experimental results vs. the FE simulations. The results of the FE models show very good accuracy. LJ-1 and LJ-2 failed in plate tear-out, as shown in Figs. 25(a) and 25(c). However, after adding the effect of thermal creep to the bolt materials in ABAQUS (2014), the failure mode changed to bolt shear failure, as shown in Figs. 25(b) and 25(d). Additionally, LJ-3 failed in bolt shear, and adding the effect of thermal creep decreased the ultimate strength capacity by 27.6%, as shown in Table 6. This proves that adding the effect of thermal creep to bolted lap

joints lead to more conservative results and prediction of the behavior and failure modes of bolted lap joints and shear tab connections.

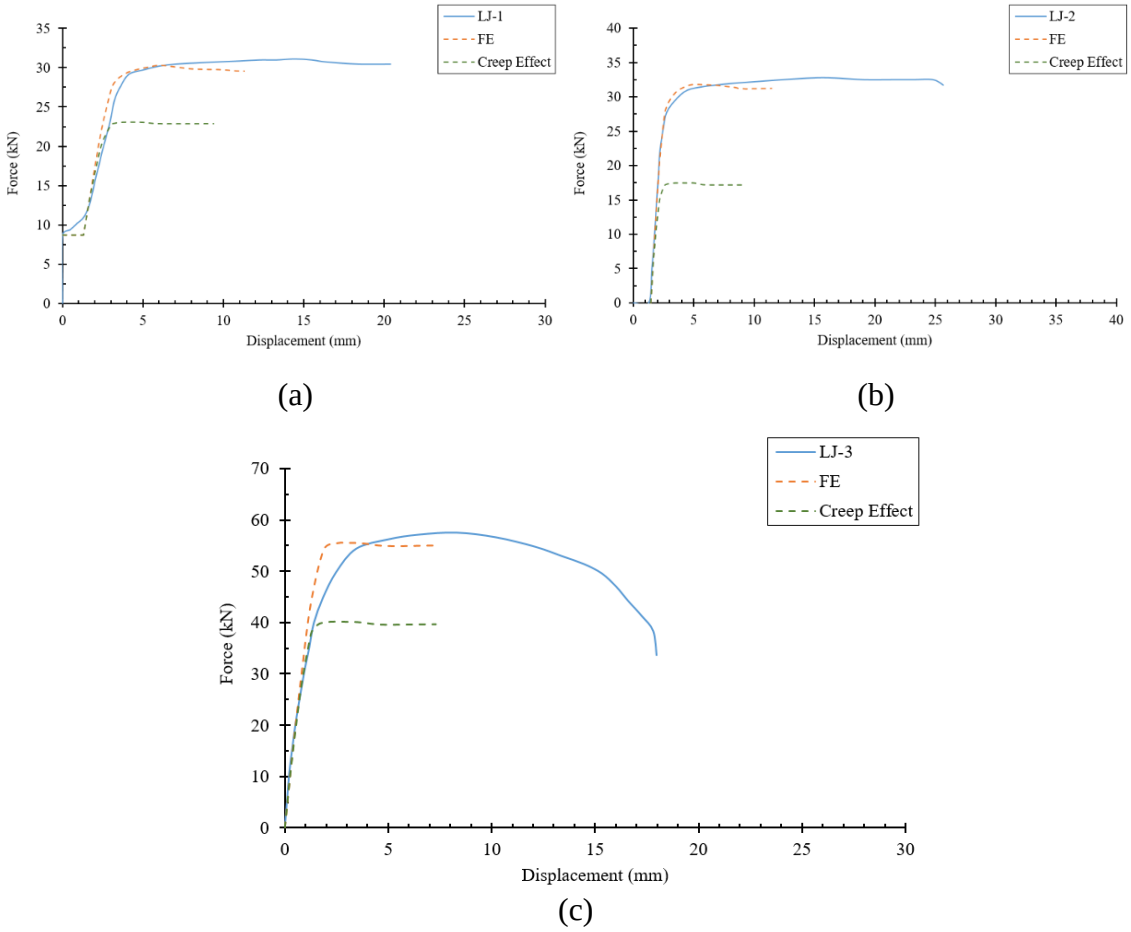

Figure. 24. Load-Displacement Validations and effect of creep at 600°C: (a) LJ-1, (b) LJ-2, (c) LJ-3

Table. 6. FE results for the effect of thermal creep on single-bolted lap joints strength capacity and failure mode

Test Name	Bolt Diameter (mm)	Plate Thickness (mm)	Failure Load, P (kN)	Failure Load, P (kN) (creep effect)	Failure Mode	Failure Mode (creep effect)	Capacity Decrease (%)
LJ-1	19	6.35	30.2	23.0	Tear-out	Bolt Shear	-
LJ-2	22.2	6.35	31.8	17.4	Tear-out	Bolt Shear	-
LJ-3	19	9.5	55.5	40.1	Bolt Shear	Bolt Shear	27.6

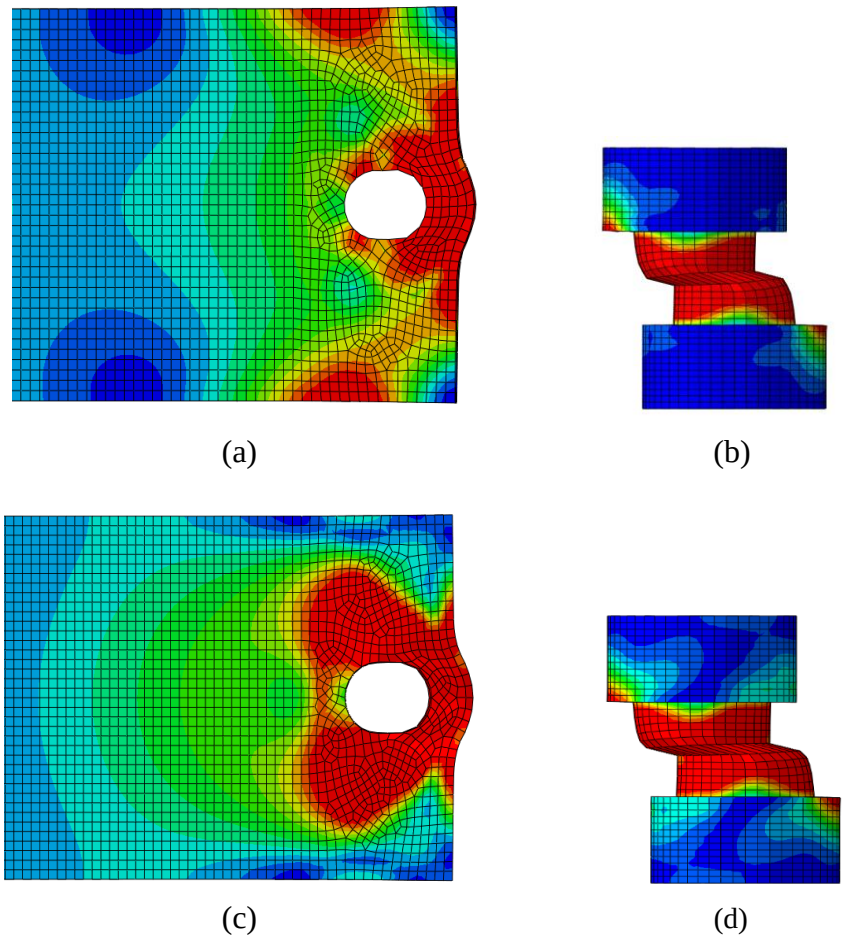

Figure. 25. FE Results at 600°C using LJ-1: (a) Base plate tear-out before creep effect, (b) bolt shear failure after creep effect, and using LJ-2: (c) Base plate tear-out before creep effect, (d) bolt shear failure after creep effect

CHAPTER V

DESIGN EXAMPLE PROCEDURE

A. Fire Design Example of an Isolated Shear Tab Connection

A step-by-step fire design procedure and an example of isolated shear tab connections are performed by referring to a design previously performed (Hantouche et al. 2020). This design incorporates the effect of thermal creep by adding the strength reduction coefficient in the bolts capacities developed in this research. The controlling failure mode of the connection is bolt shear failure, and thus the effect of thermal creep is added only in the bolt materials. The procedure is explained by designing an isolated shear tab connection. Some assumptions are made to propose a simple fire design guideline that can be applied by structural-fire engineers. The example shows the different key aspects in designing shear tab connections under elevated temperatures.

B. Design Criteria

The goal of the provided example is to design an isolated shear tab connection during fire while considering the effect of thermal creep. The connection maintains the load transfer between the beam and the column until failure occurs. When designing simple steel connections at elevated temperatures, the loads considered are namely: gravity loads, thermal-induced forces that develop due to restrained thermal expansion, and the moment demand exerted on the connection due to material degradation and sagging of the beam.

The connection considered is subjected to 500°C under steady-state temperature conditions. The connection is considered uniformly heated. The connection configuration is shown in Fig. 26.

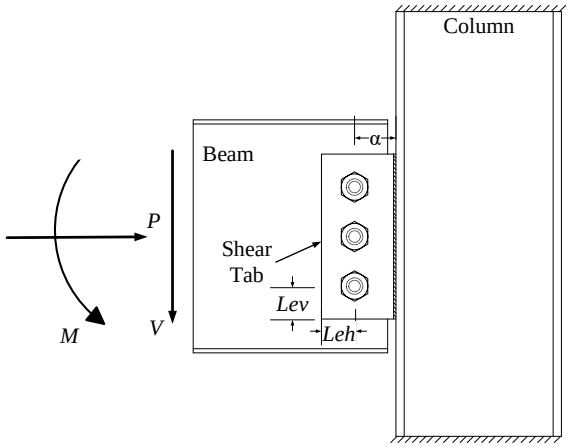

Figure. 26. Configuration of the isolated shear tab connection

C. Design Steps and Analysis Procedure

First, the connection is designed at ambient temperatures under gravity loads to meet both the serviceability and the strength requirements as per AISC *Specifications* (2016) structural design code. Then, all limit states of the connection are checked at elevated temperature. To predict the steel material properties at elevated temperatures, retention factors available in the AISC *Appendix 4* (2016) are used for the base, bolts, and weld materials. The retention factors at 20°C and at 500°C are presented in Table 7. Then, Equation (2) is used to calculate the bolt strength capacities at elevated temperatures which considers the effect of thermal creep. The applied gravity load is assumed as an applied shear force (V), the thermal induced forces are assumed as a tension force (P), and the applied moment demand is assumed as a moment rotation (M).

Table. 7. Material Properties Retention Factors available in AISC 360 Appendix 4 (2016)

Retention Factor	Temperature	
	20°C	500°C
Base material yield strength (K_{yt})	1	0.6
Base material ultimate strength (K_{ut})	1	0.78
Bolt ultimate strength (K_{bt})	1	0.54
Weld ultimate strength (K_{wt})	1	0.627

D. Design Example

1. Given:

An isolated shear tab connection composed of W16x40 unprotected steel beam section and W10x49 column section, as shown in Fig. 26. The beam, column, and shear tab plates are of S355 steel material. The weld material is E70XX. The beam is connected to the shear tab through a single column of three Grade 10.9 X-shear bolts having a diameter of 1 in. The setback distance is 0.5 in. The beam and the connection are uniformly heated to 500 °C. The beam is assumed to carry a shear force of 40 kips due to gravity loads, and an axial force of 15 kips due to thermal expansion of the beam at 500°C. Also, the connection is assumed to be subjected to a moment of 15 kips-inch. The connection will be analyzed before and after adding the thermal creep effect on the shear tab connection.

2. Solution

Step 1: Shear Tab Connection Configuration

Setback distance = 0.5 in.: $a \le 3\frac{1}{2}$ in. Take $a = 2\frac{1}{2}$ in.

The horizontal edge distance of the plate $L_{eh} \ge 2d_b = 1.75$ in. Take $L_{eh} = 2$ in.

The vertical edge distance, L_{ev}, according to Table J3.4 in the AISC *Specifications* (2016), has a minimum value of 1 in. for bolt diameter of ¾ in. Take $L_{ev} = 2$ in.

The eccentricity $e = \frac{a}{2} = 1\frac{1}{4}$ in.; according to Table 10-9 in the AISC *Steel Construction Manual* (2017).

The maximum thickness of the connecting plate: $t_{\max} = \left(\frac{d_b}{2} + \frac{1}{16}\right) = 0.4375$ in. Take $t = \frac{5}{16}$ in. according to Table 10-9 in the AISC *Steel Construction Manual* (2017)

The minimum length of the plate should be greater than half the height of the beam web (7.5 in). Therefore, the plate length is 10 in. and the bolts vertical spacing is 3 in.

For $t = \frac{5}{16}$ in., fillet weld thickness $w_{\min} \ge \frac{3}{16}$. Let thickness $w = \frac{1}{4}$ in., according to AISC *Specifications* (2016).

The horizontal edge distance of the beam is equal to $a - 0.5 = 2\,\text{in.}$

Step 2: Check the Beam Strength Capacity

Check beam shear strength:

Given shear force applied:

$V = 40\,\text{kips}$

The shear yielding capacity of the beam:

$$\begin{aligned} 0.6K_{yt}F_{yt}A_s &= 0.6(0.6)(50\,\text{ksi})(16\,\text{in.})(0.305\,\text{in.}) \\ &= 87.84\,\text{kips} > 40\,\text{kips} \end{aligned}$$

Step 3: Compute the Applied Shear Force on the Bolts

The shear tab is connected to the beam web by one column of three shear bolts.

Step 3a – Bolt shear force due to gravity load

$$\begin{aligned} V_v &= \frac{V}{3} \\ &= \frac{40\,\text{kips}}{3} \\ &= 13.33\,\text{kips/bolt} \end{aligned}$$

Step 3b – Bolt shear force due to thermal expansion

$$\begin{aligned} V_p &= \frac{P}{3} \\ &= \frac{15\,\text{kips}}{3} \\ &= 5\,\text{kips/bolt} \end{aligned}$$

Step 3c – Bolt shear force due to the applied moment on the connection

$$\begin{aligned} V_m &= \frac{M}{2p} \\ &= \frac{15\,\text{kip-in.}}{6\,\text{in.}} \\ &= 2.5\,\text{kips/bolt} \end{aligned}$$

Step 3d – Applied shear force on each bolt

$$\begin{aligned} V_{top} &= \sqrt{(V_M - V_P)^2 + (V_v)^2} \\ &= \sqrt{(2.5\,\text{kips} - 5\,\text{kips})^2 + (13.33\,\text{kips})^2} \\ &= 13.56\,\text{kips} \end{aligned}$$

$$\begin{aligned} V_{middle} &= \sqrt{(V_P)^2 + (V_v)^2} \\ &= \sqrt{(5\,\text{kips})^2 + (13.33\,\text{kips})^2} \\ &= 14.23\,\text{kips} \end{aligned}$$

$$V_{bottom} = \sqrt{(V_M + V_P)^2 + (V_v)^2}$$
$$= \sqrt{(2.5\text{ kips} + 5\text{ kips})^2 + (13.33\text{ kips})^2}$$
$$= 15.29\text{ kips}$$

Step 4: Slip-Critical Capacity at Elevated Temperature

To determine the slip-critical capacity of the shear tab connection at 500°C, Equation (1) is used and incorporated in equation (J3-4) available in the AISC 360 *Specifications* (2016):

$$k_{PT} = -0.0009T + 0.692$$
$$= -0.0009(500) + 0.692$$
$$= 0.242$$

$$R_n = \mathrm{k}_{PT}\mu \mathrm{D}_u h_f T_b n_s$$
$$= 0.242(0.3)(1.13)(1.0)(28)(1.0)$$
$$= 2.3\text{ kips}$$

Step 5: Determine the Strength of the Shear Tab Plate

Step 5a – Shear yielding

$$R_{vy} = 0.6K_{yt}F_{yt}A_s$$
$$= 0.6(0.6)(50\text{ ksi})(3.75\text{ in.}^2)$$
$$= 67.5\text{ kips} > V$$

Step 5b – Shear rupture

$$R_{vu} = 0.6K_{ut}F_{ut}A_{s,net}$$
$$= 0.6(0.78)(65\text{ ksi})(2.48\text{ in.}^2)$$
$$= 75.44\text{ kips} > V$$

Step 5c – Flexural yielding

$$M_y = K_{yt}F_{yt}Z_x$$
$$= 0.6(50\text{ ksi})(9.375\text{ in.}^3)$$
$$= 281.25\text{ kip-in.} > M$$

Step 5d – Flexural rupture

$$M_u = K_{ut}F_{ut}Z_{net}$$
$$= (0.78)(65\text{ ksi})(2.58\text{ in.}^3)$$
$$= 130.91\text{ kip-in.} > M$$

Step 5e – Block shear

$$R_{bs} = U_{bs}A_{nt}K_{ut}F_{ut} + \min\begin{bmatrix} 0.6A_{nv}K_{ut}F_{ut} \\ 0.6A_{gv}K_{yt}F_{yt} \end{bmatrix}$$

$$A_{nt} = [2\text{ in.} - 0.5(1.125\text{ in.})](\tfrac{3}{8}\text{ in.})$$
$$= 0.539\text{ in.}^2$$

$$A_{gv} = 8\text{ in.}(\tfrac{3}{8}\text{ in.})$$
$$= 3.0\text{ in.}^2$$

$$A_{nv} = [8\text{ in.} - 2.5(1.125\text{ in.})](\tfrac{3}{8}\text{ in.})$$
$$= 1.95\text{ in.}^2$$

$$0.6A_{nv}K_{ut}F_{ut} = 0.6(1.95\text{ in.}^2)(0.78)(65\text{ ksi})$$
$$= 59.32\text{ kips}$$

$$0.6A_{gv}K_{yt}F_{yt} = 0.6(3.0\text{ in.}^2)(0.6)(50\text{ ksi})$$
$$= 54.0\text{ kips}$$

$$R_{bs} = 1(0.539\text{ in.}^2)(0.78)(65\text{ ksi}) + 54.0\text{ kips}$$
$$= 81.33\text{ kips} > V$$

Step 6: Determine the Strength of Welds and Bolts

Step 6a – Weld strength

$V = 40\text{ kips}$

$$f_v = \frac{40\text{ kips}}{2(10\text{ in.})}$$
$$= 2\text{ kip/in.}$$

The moment applied to the weld is:

$$M + Ve = 20\text{ kip-in.} + 40\text{ kips}(1.25\text{ in.})$$
$$= 70\text{ kip-in.}$$

Maximum stress perpendicular to the weld is:

$$f_t = \frac{(M + Ve)h}{4(I_{weld})}$$
$$= \frac{12(70\text{ kip-in.})(10\text{ in.})}{4(10\text{ in.})^3}$$
$$= 2.1\text{ kip/in.}$$

Therefore, the maximum resultant force is: $\sqrt{(2.1\text{kip/in.})^2 + (2\text{ kip/in.})^2} = 2.9\text{ kip/in.}$

$$\tan\theta = \frac{f_t}{f_v}$$
$$= \frac{2.1\text{kip/in.}}{2\text{ kip/in.}}$$

$$\theta = 46.4^\circ$$

$$R_{nw} = 0.6K_{wt}F_{EXX}(1+0.5\sin^{1.5}\theta)A_{we}$$
$$= 0.6(0.627)(70\text{ ksi})\left[1+0.5\sin^{1.5}(46.4^{\circ})\right](0.707)(\tfrac{1}{4}\text{ in.})$$
$$= 6.1\text{ kip/in.} > 2.9\text{ kip/in.}$$

Step 6b – Shear tab bearing and tear-out resistance

$$R_{br} = 2.4K_{ut}F_{ut}d_b t \le 1.2l_c tK_{ut}F_{ut}$$
$$= 3.0(0.78)(65\text{ ksi})(1\text{ in.})(\tfrac{3}{8}\text{ in.}) \le 1.2(1.438\text{ in.})(\tfrac{3}{8}\text{ in.})(0.78)(65\text{ ksi})$$
$$= 32.8\text{ kips/bolt}$$

Step 6c – Beam bearing and tear-out resistance

$$R_{br} = 2.4K_{ut}F_{ut}d_b t \le 1.2l_c tK_{ut}F_{ut}$$
$$= 3.0(0.78)(65\text{ ksi})(1\text{ in.})(0.305\text{ in.}) \le 1.2(1.438\text{ in.})(0.305\text{ in.})(0.78)(65\text{ ksi})$$
$$= 26.67\text{ kips/bolt}$$

Step 6d – Bolt shear strength

Before adding the thermal creep effect:

$$R_v = K_{bt}A_bF_{nv}$$
$$= (0.54)(68\text{ ksi})\left[\frac{\pi(0.75\text{ in.})^2}{4}\right]$$
$$= 16.21\text{ kips/bolt}$$

After adding the thermal creep effect:

The strength reduction coefficient is calculated using Equation (3):

$$\alpha = -0.0014\text{T} + 1.3$$
$$= -0.0014(500°\text{C}) + 1.3$$
$$= 0.6$$

The bolt shear strength capacity after adding the effect of thermal creep is then calculated using Equation (2):

$$R_v = \alpha K_{bt}A_bF_{nv}$$
$$= 0.6(0.54)(64\text{ ksi})\left[\frac{\pi(0.75\text{ in.})^2}{4}\right]$$
$$= 9.72\text{ kips/bolt}$$

Compare the strength values of bolts in shear, shear tab in bearing and tear-out, and beam web in bearing and tear-out. The capacity of the beam web in tear-out has the minimum strength.

$V_{top} = 13.56\text{ kips} < R_{v,bolt}$ (OK)

$V_{middle} = 14.23\text{ kips} < R_{v,bolt}$ (OK)

$V_{bottom} = 15.29 \text{ kips} < R_{v,bolt}$ (OK)

The limit state capacities are shown in Table 8. As shown, the isolated shear tab connection is expected to fail in bolt shear. Using the assumed loads applied, the connection does not fail since the force does not reach the bolt shear resistance. However, after adding the effect of thermal creep to the bolt capacity equation, the connection capacity decreases by 40% and the connection fails in bolt shear due to the applied loads. This shows that neglecting the effect of thermal creep leads to unsafe predictions of behavior, strength capacities and failure mode of shear tab connections subjected to elevated temperature. The final geometric configuration of the shear tab connection is shown in Fig. 27.

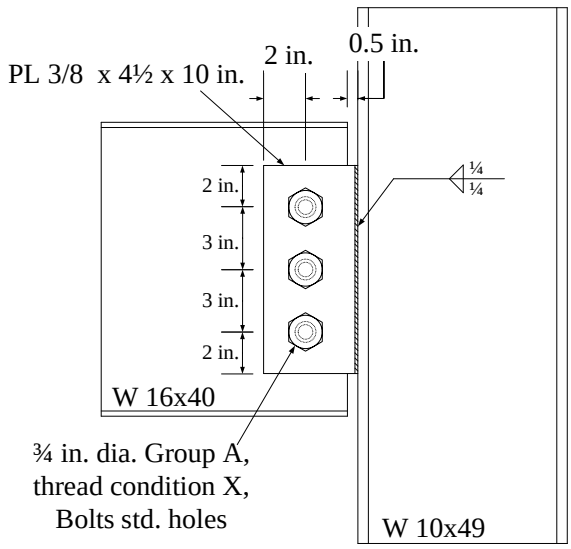

Figure. 27. Detailed sketch design for isolated shear tab connection

Table. 8. Summary of Limit state capacities for shear tab connection at 500°C

Limit State	Capacity
Flexural yielding of plate	281.25 kips
Flexural rupture of plate	130.91 kips
Block shear of plate	81.33 kips
Shear rupture of plate	75.44 kips
Shear yielding of plate	67.5 kips
Weld strength	6.1 kips/in.
Shear tab bearing and tear-out resistance	32.8 kips/bolt
Beam bearing and tear-out resistance	26.67 kips/bolt
Bolt shear strength before thermal creep effect	16.21 kips/bolt
Bolt shear strength after thermal creep effect	9.72 kips/bolt

CHAPTER VI

SUMMARY, CONCLUSIONS AND RECOMMENDATIONS

A. Summary and Conclusions

This research investigates the rate- and temperature-dependent behavior of single-shear bolted lap joints under elevated temperatures. Sixteen bolted lap joints are tested under two loading rates, fast (1.5 mm/min) and slow (0.1 mm/min), for temperatures ranging from 400°C to 700°C with 50°C increment using steady-state temperature conditions. The purpose of the experimental program is to show the influence of loading rates or implicit creep on the bolted lap joint strength capacities, deformations, and pretension force of Grade 8.8 bolt. Also, this study helps in understanding the rate-dependent behavior of bolts subjected to shear forces and their implications on bolted connections at high temperatures to ensure a safe design. Then, FE simulations are performed to validate the experimental program performed and others available in the literature. The models show the effect of implicit creep on previously performed shear tab connections failure modes, strength capacities, and rotations at elevated temperatures. Finally, a step-by-step fire design procedure and an example is performed on an isolated shear tab connection at 500°C that shows the effect of incorporating the developed strength reduction coefficient in the bolt shear capacity. The following conclusions from this study are derived:

- The tested specimens failed due to bolt shear failure at temperatures ranging from 20°C to 700°C under both loading rates.
- The failure behavior shifted from brittle to ductile at around 500°C and limited hole ovalization was observed under all temperatures and both loading rates, indicating no change in failure mode.

- As temperature increases, the bolt shear strength capacity, and the initial stiffness decrease. That is, as temperature increases to 700°C, the reduction of the bolt shear strength reaches its ultimate of 89% and 92% decrease for the fast and slow rates, respectively.
- The axial displacement increases as temperature increases, indicating that the bolted lap joint behaves in a more ductile behavior when subjected to higher temperatures.
- An equation is proposed that calculates the retention factors of the minimum bolt pretension force for Grade 8.8 M20 X-bolts. These retention factors can be used in the slip-resistance design equation of bolted connections to predict slip-critical capacities for temperatures ranging from 400°C to 700°C.
- No major effect of loading rate on neither the bolt pretension force nor the initial stiffness, indicating that the inelastic creep strains are insignificant for low load levels.
- The effect of loading rate significantly initiates at 450°C with 18% decrease in strength capacity till it reaches its ultimate with 36% decrease at 700°C.
- The tests show a similar strength capacity for those performed at 650°C and 700°C under slow and fast loading rates, respectively.
- The retention factors obtained using the slow loading rate tests result in a more conservative bolt shear capacity design in bolted connections exposed to fire as compared to those using the fast tests and others available in the literature.

- Proposed values for a strength reduction coefficient, α, are used in the bolt shear capacity fire design equation. The modified equation can help predict more conservative bolt shear strength capacities at elevated temperatures while including the effect of implicit creep or loading rate.
- The value α is incorporated in the bolts materials of the FE validations to show the effect of thermal creep on shear tab connections available in the literature. This effect results in a drastic decrease of the connections bolt strength capacities and changes the failure modes from plate tear-out or block shear of the beam web to bolt shear failure at elevated temperatures.
- The designed isolated shear tab is expected to fail in bolt shear at 500°C before adding the effect of thermal creep. After incorporating the value α in the bolt shear capacity equation, the strength capacity of the shear tab connection decreases by 40%. This shows that neglecting the effect of thermal creep results in unsafe predictions of shear tab connections capacities and failure mode during a fire.

B. Recommendations

Future work should be conducted to fully comprehend the effect of thermal creep phenomena on bolted connections at elevated temperatures. The following future works are recommended:

- Testing different materials and failure modes under higher temperatures while using different loading rates are essential to develop new design guidelines for structural fire-engineering applications on bolted connections while considering the effect of rate or time.

- Performing full scale beam-column connections design which also considers the effect of creep in the base materials.
- Adding tensile and residual stresses in the design during the cooling phase of fire should be also studied to ensure the survival of the structure.
- Implementing additional load demands that accounts for the tension stresses due to beam catenary action during the later stages of fire.
- Developing a thermal creep model that accounts for the effect of loading rate on the behavior of shear tab connections in fire.

BIBLIOGRAPHY

Abaqus, V. (2014). 6.14 Documentation. *Dassault Systemes Simulia Corporation*, *651*, 6-2.

Construction, A. I. (2017). Steel construction manual. *American Instutute of Steel*.

ANSI, B. (2016). AISC 360-16, Specification for Structural Steel Buildings. *Chicago AISC*.

Boresi, A. P., Schmidt, R. J., & Sidebottom, O. M. (1993). *Advanced mechanics of materials*, *6*. New York: Wiley.

European Committee for Standardization CEN, Eurocode 3 (2005). Design of steel Structures- Part 1-2; 10 BS EN 1993-1-2, General Rules-Structural Fire Design.

Fischer, E. C., Varma, A. H., & Zhu, Q. (2018). Experimental evaluation of single-bolted lap joints at elevated temperatures. *Journal of Structural Engineering*, *144*(1), 04017176.

Garlock, M. E., & Selamet, S. (2010). Modeling and behavior of steel plate connections subject to various fire scenarios. *Journal of Structural Engineering*, *136*(7), 897-906.

Guo, Z., Lu, N., Zhu, F., & Gao, R. (2017). Effect of preloading in high-strength bolts on bolted-connections exposed to fire. *Fire Safety Journal*, *90*, 112-122.

Hantouche, E., Al Khatib, K., & Jabotian, H. V. (2020). Design of Simple Steel Connections under Fire Temperatures. *Engineering Journal*, *57*(3), 145-178.

Hanus, F., Zilli, G., & Franssen, J. M. (2011). Behaviour of Grade 8.8 bolts under natural fire conditions—Tests and model. *Journal of Constructional Steel Research*, *67*(8), 1292-1298.

Hirashima, T., Esaki, Y., & Ando, S. (2014). Load-deformation behavior of bolted double-splice friction joints at elevated temperature. In *Proceedings of 8th International Conference on Structures in Fire*. 819-826.

Hu, G., & Engelhardt, M. (2012). Studies on the behavior of steel single-plate beam end connections in a fire. *Structural engineering international*, *22*(4), 462-469.

Jabotian, H. V., & Hantouche, E. G. (2019). Thermal creep behavior of shear tabs in fire using modified burgers model. *Journal of Constructional Steel Research*, *160*, 528-539.

Kirby, B. R. (1995). The behaviour of high-strength grade 8.8 bolts in fire. *Journal of Constructional Steel Research*, *33*(1-2), 3-38.

Kodur, V. K. R., & Dwaikat, M. M. S. (2010). Effect of high temperature creep on the fire response of restrained steel beams. *Materials and structures*, *43*(10), 1327-1341.

Kodur, V., Kand, S., & Khaliq, W. (2012). Effect of temperature on thermal and mechanical properties of steel bolts. *Journal of Materials in Civil Engineering*, *24*(6), 765-774.

Matar, M. (2014). Primary creep in ASTM A325 bolts under simulated fire loading. Masters Dissertation, The University of Wisconsin-Milwaukee.

NIST, N. (2008). 1A: Final Report on the Collapse of World Trade Center Building 7. *National Institute of Standards and Technology, Gaithersburg, USA*.

Peixoto, R. M., Seif, M. S., & Vieira Jr, L. C. M. (2017). Double-shear tests of high-strength structural bolts at elevated temperatures. *Fire safety journal*, *94*, 8-21.

Seif, M. S., Main, J. A., & McAllister, T. P. (2013, April). Performance of steel shear tab connections at elevated temperatures. In *Proceedings of the Annual Stability Conference, Structural Stability Research Council, St. Louis, Missouri*. 16-20.

Seif, M., Main, J., Weigand, J., McAllister, T. P., & Luecke, W. (2016, May). Finite element modeling of structural steel component failure at elevated temperatures. In *Structures*, 6, 134-145. Elsevier.

Torić, N., Harapin, A., & Boko, I. (2013). Experimental verification of a newly developed implicit creep model for steel structures exposed to fire. *Engineering Structures*, *57*, 116-124.

.

Yang, K. C., Hsu, R. J., & Chen, Y. J. (2011). Shear strength of high-strength bolts at elevated temperature. *Construction and Building Materials*, *25*(8), 3656-3660.

Yu, H., Burgess, I. W., Davison, J. B., & Plank, R. J. (2009). Experimental investigation of the behaviour of fin plate connections in fire. *Journal of Constructional Steel Research*, *65*(3), 723-736.

Yu, L. (2006). Behavior of bolted connections during and after a fire (Doctoral dissertation). University of Texas, Austin, TX.